Femtosecond Studies of Solvation and Intramolecular Configurational Dynamics of Fluorophores in Liquid Solution

Max Glasbeek* and Hong Zhang

Laboratory for Physical Chemistry, University of Amsterdam, Nieuwe Achtergracht 129, 1018 WS Amsterdam, The Netherlands

Received May 12, 2003

Contents

1. Introduction 1929
2. Pump–Probe and Time-Gated Fluorescence Up-Conversion Techniques 1931
3. Deactivation of Electronically Excited Organic Chromophore (Dye) Molecules 1933
   3.1. Solvation Dynamics 1933
      3.1.1. Introduction 1933
      3.1.2. Styryl Dyes 1934
      3.1.3. Coumarins 1942
      3.1.4. Organic Light-Emitting Diode (OLED) Dyes 1943
   3.2. Intramolecular Twisting Dynamics 1945
      3.2.1. Auramine 1945
      3.2.2. Two-Dimensional Dynamics: Michler's Ketone 1947
      3.2.3. Coumaric Acid in Solution and Proteins 1949
4. Concluding Remarks 1951
5. References 1951

1. Introduction

Fluorescent chromophores are optically active probe molecules with widespread applications in chemistry and biology. Usually chromophores function in condensed matter (liquid solution, protein environment, thin film, etc.), and their optical properties are strongly influenced by the medium. Chromophore−solvent interactions may be static or dynamic in nature or both. Generally, static properties, such as electronic energy, dipole moment, and molecular configuration, vary with the electronic state of the chromophore and conventional continuous wave optical spectroscopy is quite adequate for disclosing many characteristics of the static chromophore−solvent interactions.[1−5] Knowledge obtained from these spectroscopic investigations is not only of scientific interest but also of great value for the development of a large variety of molecular devices. Examples include chemosensors,[6−13] chiroptical and molecular switches,[14−19] optoelectronic devices (e.g., LED, displays, organic lasers, light detectors, solar cell materials, optical memories, etc.[20−22]), and electrogenerated luminescence or electroluminescent devices.[23−27]

* Corresponding author. Phone: +31 20 525-6996. Fax: +31 20 525-6994. E-mail: glasbeek@science.uva.nl.

In addition to "static" effects, the interactions between the chromophore and the environment may lead to "dynamic" effects. In liquid (or protein) environment, the chromophore molecules may exchange energy and momentum with molecules of the medium. Of great interest to photochemistry is the dynamic response of the solvent molecules to photoinduced changes in the charge distribution of the chromophore molecules. This dynamic response of the solvent molecules is not instantaneous. The finite time for the environmental changes is crucial in determining the dynamics of the excited-state relaxation of the chromophore itself. The processes involved are generally quite complex, and their dynamics are controlled by both intra- and intermolecular interactions. Relaxation studies of photoexcited chromophores might contribute to a better insight in a wide variety of phenomena of fundamental interest. These phenomena include electronic charge redistribution,[28−34] electron and proton transfer,[28−40] (large amplitude) intramolecular torsional motions,[41] trans−cis isomerization,[42,43] intramolecular vibrational redistribution and intermolecular vibrational relaxation (vibrational cooling),[44−47] internal conversion,[48−52] solvation,[28−34,53−56] and so on. Typically, the time scales of these relaxation processes extend from tens of femtoseconds to hundreds of picoseconds. In the past decades, much progress in the experimental investigation of such dynamic molecular processes has been achieved. It is fair to say that to a large extent these studies have only been possible because of the rapid developments in the technology for generating ultrashort laser pulses.[57−59] Presently, ultrashort laser pulses of duration of 30 fs or less, from the ultraviolet to the far-infrared, are commercially available. Together with the technological developments, a broad variety of nonlinear optical pulse methods were devised, thus allowing many new perspectives for the detailed mapping of intra- and intermolecular interactions.[60] The new information gathered from ultrafast molecular spectroscopic research also has led to a flurry of quantum mechanical treatments of chemical reactions.[60−62]

In this paper, we present a comprehensive review of ultrafast studies of large-sized fluorophores in liquid solution performed in the past decade using the femtosecond fluorescence up-conversion technique (section 2). Femtosecond transient absorption results relevant for better understanding of the up-conversion results of some of the chromophores have

10.1021/cr0206723 CCC: $48.50
Published on Web 03/11/2004

Max Glasbeek has worked in the field of molecular spectroscopy since he received his Ph.D. in 1969 at the University of Amsterdam, The Netherlands. He has been guest research scientist at the University of California at Berkeley, the California Institute of Technology, and the Australian National University in Canberra. In 1988, he was appointed John van Geuns professor in Molecular Spectroscopy at the University of Amsterdam, and since 1993, he has been full professor of Physical Chemistry at the same university. His research interests include ultrafast solvation dynamics and intramolecular excited-state twisting/charge transfer dynamics in the condensed phase.

Hong Zhang obtained his B.Sc. degree in physics at the University of Science and Technology of China (USTC) in Hefei, China, in 1985 and his M.Sc. degree at the Changchun Institute of Physics, China, in 1988. His Ph.D. research was on picosecond spectroscopy of multiple quantum well systems and was carried out under the guidance of Professors Goovaerts and Schoemaker at the University of Antwerp, Belgium. In 1993, he joined the group of Prof. Glasbeek at the University of Amsterdam as a postdoctoral fellow. His current position is assistant professor, and his main research interests are ultrafast dynamics in condensed phase and nonlinear spectroscopic techniques.

been included. It is hoped that the review gives a perspective of how femtosecond fluorescence upconversion experiments can be utilized to disentangle the contributions of intramolecular interactions (torsional or twisting dynamics, but also in a few cases, internal conversion, intramolecular vibrational redistribution, vibrational cooling)[63,64] on one hand and solvation dynamics on the other hand in excited-state relaxation of large molecules with great potential for applications in different fields.

After the excitation of an electronic state of a large-sized solute molecule in solution, various competitive processes contribute to the relaxation of the system. Figure 1 is illustrative of the schemes most often used to discuss the processes. Figure 1a depicts the typical behavior of the free energies of electronic ground and

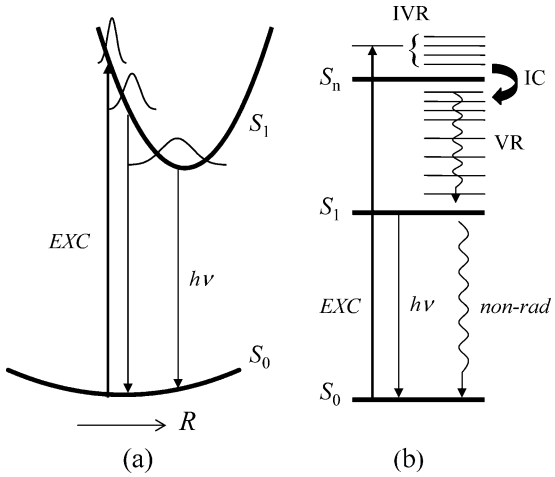

Figure 1. Schemes of excited-state relaxation (a) free energies of ground and first excited states as a function of generalized reaction coordinate (R) and (b) intramolecular relaxation processes. IC denotes internal conversion; IVR, intramolecular vibrational relaxation; VR, vibrational relaxation; and *non-rad*, nonradiative decay.

excited states of a system as a function of a generalized reaction coordinate; Figure 1b displays a diagram of the possible molecular relaxation pathways (internal conversion (IC), intramolecular vibrational relaxation (IVR), vibrational relaxation to thermalize with the bath (VR), radiative and nonradiative decay). Key topics of interest in studies of chemical reaction dynamics are (i) the relaxation pathway(s) relevant for the system under investigation, (ii) the dynamics characteristic of the various steps involved, (iii) the physical origin of the mode(s) that are represented by the generalized reaction coordinate(s) (solvent reorientational modes, conformational modes, etc.), and (iv) the functional shape of the (multidimensional) free energy surface involved in the reaction. A major practical problem in studies of large-sized molecules in condensed matter is that dark processes such as IC, IVR, and solvation occur on an ultrafast time scale and thus very often are difficult to distinguish from each other. This poses a tremendous challenge to the experimentalist in establishing the various contributions of the different steps in the relaxation process.

The considered chromophores show fast (femtosecond−picosecond) transient fluorescence behavior and are crudely divided in two categories, depending on whether the fastest transient components are determined by intermolecular or intramolecular interactions. Chromophores of the first category show *solvation dynamics*. Solvation dynamics arises from intermolecular solute−solvent interactions that convey the kinetics of the rapid motions of the solvent molecules to the fluorescent probe molecules. In chromophores of the second category, *intramolecular configurational* (*twisting*) modes, often in combination with solvation modes, control the dynamics of the fastest components in the fluorescence of the chromophore. In this category, we include also examples of chromophores for which the contributions of intramolecular twisting and solvation to the fluorescence dynamics of the chromophore can be treated on equal footing.

Especially chromophores with emissive charge transfer (CT) states, characterized by a large electric dipole moment, have served as prototype molecules in studies of solvation dynamics. In polar solvents, these chromophores give rise to large solvatochromic effects; that is, the CT-state band emission shows an appreciable Stokes (red) shift (often in excess of several thousand wavenumbers) when solvation takes place. The dynamics of solvation is intimately related to the dynamics of the solvent molecular motions. Time-dependent Stokes shift measurements provide valuable information regarding molecular dynamics in liquids. The Stokes-shift time dependence is related to dielectric relaxation dynamics, which originates from the electrostatic interactions between the charge (dipole) of the solute with the surrounding polar solvent molecules and which gives rise to a frequency dependence of the dielectric relaxation.[65−72] In this paper, however, emphasis is on experiment rather than theory.

In studies of solvation dynamics the fluorescent probe molecules must fulfill certain requirements: the probe molecules must be chemically inert with respect to the solvent, and also, the dynamic Stokes shift must be predominantly (exclusively) due to the solvation process. Hence, time-resolved solvation dynamics studies of large molecules comprise (a) verification of these requirements and (b) the measurement of the time dependence of the absorption/emission spectrum following short-pulse excitation.

For molecules of the second category considered here, electronic excitation leads to intramolecular *configurational changes* due to large amplitude torsional motions of functional groups. For some of these molecular systems, the synthesized structure may be redesigned in such a manner that the functional groups are "bridged" or bonded, and torsional or twisting motions of the functional groups become impaired. Thus the influence of bridging on the dynamics of the twisting process can be selectively investigated. Also, the solvent has great influence on the rate of the intramolecular configurational changes. Now "collisional" friction (rather than "dielectric" friction as in solvation) largely affects the isomerization or twisting dynamics. The topic of functional group twisting has long been related to intramolecular charge transfer, hence the concept of a twisted intramolecular charge transfer (TICT) state.[73−75] For many systems, the TICT phenomenon has been studied in great detail, and the results have been extensively reviewed.[4,41] However, relatively few ultrafast studies concerning TICT states have been reported, in part because TICT molecules are weakly or nonfluorescent. Results of recent ultrafast investigations on TICT molecules are included in this review.

Finally, for many large molecules, the distinct treatment of ultrafast solvation and conformational relaxation dynamics is far too simple and extreme. Due to the immense number of motional degrees of freedom, characteristics of the total system of solute and solvent molecules, solvation, and conformational relaxation often become highly competitive, and a separate treatment of their dynamics is not meaningful. We include in this review results of femtosecond fluorescence up-conversion experiments for a number of fluorophores for which solvation and intramolecular torsional dynamics are of equal importance.

The paper is organized as follows. In section 2, a brief outline is presented of the most commonly applied ultrafast spectroscopic techniques, that is, pump−probe transient absorption spectroscopy with femtosecond and picosecond time resolution and fluorescence up-conversion spectroscopy with femtosecond time resolution. Section 3 reviews recent ultrafast studies of solvation and configurational or two-dimensional solvation/torsional dynamics, as observed for various large-sized organic molecules in the fluorescent excited state. For several example chromophores, we have reproduced femtosecond fluorescence up-conversion results taken from our previous publications.

Many molecules show configurational *and* solvation dynamics, although of unequal weight. In these cases, the molecule is categorized according to which of the two is dominant for the fastest fluorescence transient component. Thus, in the category solvation dynamics, we have included results for the styryl dyes (4-(dicyanomethylene)-2-methyl-6-(*p*-(dimethylamino)styryl)-4*H*-pyran (DCM), 2-(*p*-dimethylaminostyryl)pyridylmethyl iodide (DASPI), and 6,7-benzo,3-ethyl,2-[1′,3′-butadienyl,4′-(4″-dimethylaminophenyl)] benzothiazolium perchlorate (LDS-750) because the fastest fluorescence components for these solutes in polar solvents could be shown to arise from solvation, whereas torsional or trans−cis isomerization motions are on a much slower time scale (see section 3.1). Also, for the styryl dyes dimethylaminostyryl pyridinium (DPD) and DPDO, a few IR dyes containing double bonds, and the organometal organic light-emitting diode (OLED) compound aluminum(III)-8-hydroxyquinoline (Alq_3), it could be demonstrated that solvation dynamics is faster than torsional motions (section 3.1). The diphenyl-aminomethane cation auramine O is an example of a polyphenyl methane dye for which the excited-state dynamics is dominated by intramolecular twisting (section 3.2). Section 3.2 contains in addition results for a styryl dye showing intramolecular configurational dynamics rather than solvation dynamics. The results are found for the chromophore coumaric acid, which is the active chromophore in the photocycle of photoactive yellow protein (PYP). In section 3.2, we also review the two-dimensional twisting and solvation dynamics of two analogue compounds of auramine, namely, Michler's ketone and the bridged derivative compound 3,6-bis(dimethylamino)-10,10-dimethylanthrone (BMK). Concluding remarks are presented in section 4.

2. Pump−Probe and Time-Gated Fluorescence Up-Conversion Techniques

One of the most important issues in ultrafast spectroscopic experiments is the generation of stable ultrashort laser pulses. Nowadays, mode-locked Ti:sapphire lasers can routinely provide highly stable pulses, in some laboratories even as short as about

4 fs. For the majority of the ultrafast experiments of interest in this paper, the wavelength of the pulses of the fundamental laser mode (near 800 nm) is of no practical use and spectral tunability in the UV and visible spectral region is frequently required. This is accomplished by means of an OPA (optical parametric amplifier). The OPA is pumped with amplified pulses at the fundamental or doubled frequency from the Ti:sapphire laser. Inside the OPA, these pulses are first down-converted into the infrared and then up-converted into the UV or visible spectral range. In recent years, several groups have extended the investigation of ultrafast phenomena into different spectral regions, that is, the (mid)infrared[76−81] and soft and hard X-ray range.[82−86] A further survey of these interesting developments is beyond the scope of this paper, however.

To monitor optical responses on a femtosecond or (sub)picosecond time scale, conventional electronic detection techniques, such as time-correlated single-photon-counting or streak camera detection, generally are inappropriate because with use of these techniques the time resolution will be limited by (relatively slow) electronic switches and thus measurements on a time scale corresponding to the cross-correlation time of the femtosecond laser pulses are impeded. Most ultrafast optical studies make use of a sequence of various ultrashort laser pulses. In the simplest scheme, a pump pulse excites the optically active species into a higher electronic or vibronic state and a second (probe) pulse interrogates the time evolution of the excited system. Pump−probe experiments involve the measurement of higher order polarization and thus are part of nonlinear optical spectroscopy.[60] More specifically, in case of the aforementioned pump−probe scheme, the probed optical polarization is third-order in the electric fields of the pump (second-order) and probe (first-order) pulses. The main advantage of pump−probe techniques is that the instrumental response is limited by the laser pulse duration instead of the electronic response time as in conventional pico- and nanosecond experiments.

Here we briefly outline two of the most commonly used techniques: femtosecond transient absorption/gain spectroscopy and femtosecond fluorescence up-conversion spectroscopy.

In a transient absorption/gain experiment, a pump pulse excites the optically active molecule into an electronically excited state and a probe pulse, after a preset delay, passes through the pumped sample area. The relative change of the sample transmission is normally given by $\Delta T(\omega)/T_{\mathrm{probe}}(\omega) = \{T'_{\mathrm{probe}}(\omega) - T_{\mathrm{probe}}(\omega)\}/T_{\mathrm{probe}}(\omega)$, $T'_{\mathrm{probe}}(\omega)$ and $T_{\mathrm{probe}}(\omega)$ being the transmission of the probe pulse with and without pump pulse, respectively. In principle, coherent polarization and population changes of the coupled levels contribute to the signal.[87] The coherent polarization component normally is short-lived and exists up to a few tens of femtoseconds only. After dephasing of the coherence, the $\Delta T(\omega)$ signal is generally determined by the superposition of ground-state absorption (bleaching), excited-state absorption, and stimulated emission (gain). The pump−probe technique is relatively simple and straightforward and one of the most widely applied in ultrafast spectroscopic studies.

For the study of ultrafast excited-state dynamics of fluorescent molecules, the application of the femtosecond fluorescence up-conversion technique[88−90] is often a very attractive alternative for the pump−probe method. The great advantage of this technique is that it is only sensitive to the population dynamics of the fluorescent excited state; dynamic effects due to changes of the ground-state population or excited-state absorption or both remain unobserved. This makes the technique highly selective. In the experiment, the temporal behavior of the excitation-pulse-induced fluorescence is measured by mixing the fluorescence response in a nonlinear crystal with a second laser (gate) pulse applied at a variable and controllable delay with respect to the excitation pulse. Mixing of the fluorescence with the gate pulse generates a sum-frequency signal for which the intensity is proportional to the fluorescence intensity at the delay time, τ. The intensity of the sum-frequency signal can be expressed by

$$I_{\mathrm{sum}}(\tau,\omega_{\mathrm{sum}}) \propto \int_{-\infty}^{+\infty} I_{\mathrm{fl}}(t,\omega_{\mathrm{fl}}) I_{\mathrm{laser}}(\tau - t,\omega)\, \mathrm{d}t \quad (1)$$

I_{sum}, I_{fl}, and I_{laser} denoting the transient up-conversion, fluorescence, and gated laser-pulse intensity, respectively; the sum frequency is given as $\omega_{\mathrm{sum}} = \omega_{\mathrm{fl}} + \omega$, ω_{fl} and ω denoting the fluorescence frequency and laser frequency, respectively. From expression 1, it follows that, after deconvolution with the instrumental response function, I_{sum} and I_{fl} show the same time profile, and thus, by monitoring the time evolution of the sum-frequency signal, one obtains the time dependence of the fluorescence. Figure 2 gives a schematic picture of the femtosecond fluorescence up-conversion setup used in the experiments of ref 38. Recently, the fluorescence up-conversion method was improved with a broad-band version in which the entire fluorescence band is upconverted using a single near-infrared gate pulse, thus allowing the direct monitoring of the time-resolved fluorescence spectrum without readjusting optical elements.[91]

The time resolution of the fluorescence up-conversion technique is usually no better than about 50−100 fs. If in the up-conversion experiment very short laser pulses (30 fs or shorter) would be used, the spectral width of the gate pulse would broaden to the extent that it would yield an undesired low value for the spectral resolution of the eventually measured (reconstructed) fluorescence spectrum. Experimentally, one thus has to find a compromise for optimizing the time and spectral resolution. In practice, the laser gating pulse usually is not shorter than ∼50 fs.

Time-resolved fluorescence up-conversion experiments are usually performed under "magic angle" conditions; that is, only the intensity of the emission polarized at an angle of 54.7° with respect to the polarization of the gating pulse is deteced so that the influence of the reorientational motions of the probe molecules on the emission intensity is eliminated.[92] On the other hand, additional information can be

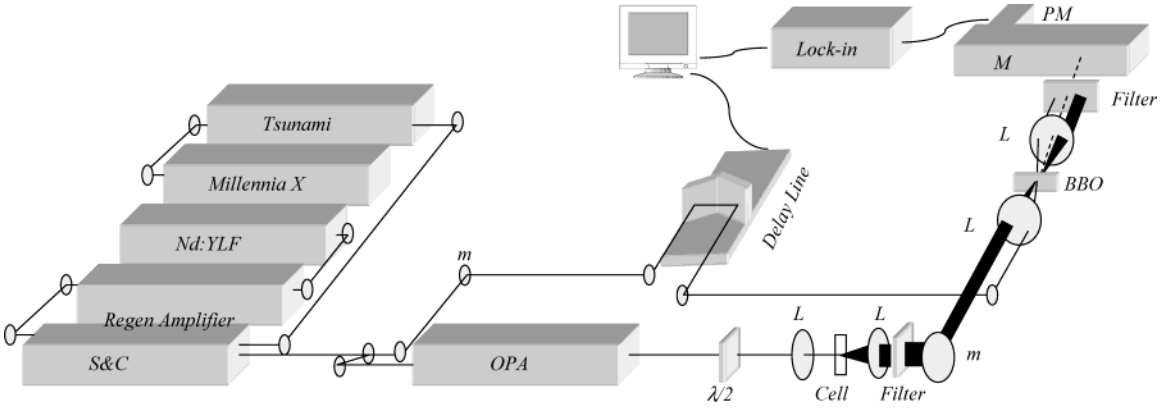

Figure 2. Schematic diagram of femtosecond fluorescence up-conversion setup.[38] On the left is the amplified laser system delivering 110 fs pulses: S&C, stretcher and compressor; OPA, optical parametric amplifier; L, lens; m, mirror; BBO, type I BBO crystal; M, monochromator; PM, photomultiplier.

obtained from time-dependent polarization measurements of up-conversion transients. Such experiments reveal the presence of rapid intramolecular excited-(electronic) state or conformational changes that cause a directional change of the optical transition moment characteristic of the fluorescence. The observable is the fluorescence anisotropy (r), defined as the normalized difference between the detected light responses polarized parallel ($I_{||}$) and perpendicular ($I_{\perp}$) to the polarization of the gating field,

$$r(t) = \frac{I_{||}(t) - I_{\perp}(t)}{I_{||}(t) + 2I_{\perp}(t)} \quad (2)$$

With neglect of the coherence components, it can readily be derived that the anisotropy of the fluorescence is given as[93]

$$r(t) = \frac{2}{5}\langle k_f(t)\rho(\omega,t)\langle P_2[\hat{\mu}_E(t)\hat{\mu}_A(0)]\rangle\rangle/\langle k_f(t)\rho(\omega,t)\rangle \quad (3)$$

where k_f, $\rho(\omega,t)$, P_2, and $\hat{\mu}_E$ and $\hat{\mu}_A$ are the radiative rate constant, the fluorescence line shape function, the second Legendre polynomial, and the unit vectors pointing in the direction of the emission and absorption dipoles, respectively, and the brackets denote the ensemble average of emissive probe molecules. Directional changes of the emission transition moment not only may be caused by the rotational diffusion motions of the optically active probe in solution but also may arise from ultrafast intramolecular processes, for example, internal conversion, charge transfer, etc. If the latter are fast enough to compete with the reorientational motions of the solute, then measurement of the rapid transient behavior of $r(t)$ may give very useful complementary information about the nature and dynamics of intramolecular relaxation processes. It may be added that ultrafast depolarization effects can also be observed in transient absorption, and in fact, such measurements proved to be very powerful for the study of ultrafast electronic dephasing.[94]

Apart from the pump−probe and fluorescence up-conversion techniques mentioned, various optical methods based on third-order nonlinear response of the ensemble of molecules have been applied for the study of the large variety of processes that may occur upon photoexcitation. These include photon echo, Kerr effect, transient grating, resonant Raman scattering, four-wave mixing, etc. An overview of these techniques can be found in ref 60.

3. Deactivation of Electronically Excited Organic Chromophore (Dye) Molecules

3.1. Solvation Dynamics

3.1.1. Introduction

Since the pioneering work of Bakshiev[95−97] and others,[98−100] time-resolved fluorescence spectroscopy has been of great importance in studies of solvation dynamics. In most experiments, ultrashort laser pulses excite (chemically inert) solute molecules into a state with an electronic charge distribution substantially different from that in the ground state. When small polar solvent molecules surround the solute molecules, following the excitation pulse the solvent molecules will rapidly reorient on account of the electrostatic solute−solvent molecular interactions, so a dynamic equilibrium in accordance with the new excited-state charge distribution of the solute is established. The usual time scale for the system to reach the new dynamic equilibrium extends from tens of femtoseconds up to the picosecond time regime. In turn, the fast reorientational motions of the solvent molecules induce a fast solvatochromic shift of the fluorescence band of the organic chromophore. The energy scheme for the process is illustrated in Figure 1a. In the figure, the free energies of the system in ground and excited states are given as a function of a generalized solvation coordinate.[28,69] It is assumed that during the (vertical) optical excitation of the chromophore, the nuclear solvent coordinates are "frozen" (Franck−Condon principle) and only the solvent electronic charge distribution can follow the photoinduced change in the chromophore electronic charge distribution. Thus, immediately after the laser pulse, the orientations of the solvent dipoles surrounding a photoexcited chromophore molecule are not (yet) adapted to the chromophore dipole moment, μ_e. Consequently, the solvent molecules are forced to reorient until a new orientational equilibrium in accordance with the direction and magnitude of μ_e is established. During

this solvation process, the free energy separation of the ground and excited states is reduced (Figure 1a); this results in a red shift of the fluorescence band (dynamic Stokes shift). Strictly speaking, the use of free energy functions in the description of nonequilibrium processes is questionable.[101] The validity of the approach may be motivated as follows, however. At each moment, we consider the orientation of the solvent dipoles surrounding the photoexcited solute molecules to be in equilibrium with an effective solute dipole moment given as

$$\mu(t) = \mu_g[1 - z(t)] + \mu_e z(t) \quad (4)$$

$\mu(t)$ being the effective dipole moment, μ_g and μ_e being the dipole moments in the ground and excited states, respectively, and $z(t)$ being the dimensionless solvation coordinate. The effective dipole moment at time t is in equilibrium with the orientational polarization of the solvent molecules and hence free energies for the system in the ground and excited state can be conceived. The effective dipole moment and the free energies of the system in the ground and excited state thus adiabatically follow the changes of the solvent polarization that accompany the reorientational motions of the solvent molecules. Since at $t \leq 0$, the effective dipole moment of the solute is μ_g, one has $z(0) = 0$; when $t = \infty$, the effective moment equals μ_e (ignoring relaxation to the ground state); hence, $z(\infty) = 1$.

Usually the observed dynamic Stokes shift is expressed as[65]

$$C_\nu(t) = \frac{\nu(t) - \nu(\infty)}{\nu(0) - \nu(\infty)} \quad (5)$$

where $C_\nu(t)$ is representative of the normalized spectral response function. In expression 5, $\nu(0)$, $\nu(t)$, and $\nu(\infty)$ represent the optical frequencies that correspond to the maxima of the emission spectra of the fluorescent chromophore at time zero, at time t, and at infinite time. Within the approach of linear response,[102,103] the time dependence of $C_\nu(t)$ equals that of the time autocorrelation function of the fluctuations in the optical transition frequency as caused by the interactions with the bath of solvent molecules.[102−106] In other words, the measurement of the time dependence of $\nu(t)$ allows the determination of the time autocorrelation function characteristic of the fluctuations in the motions of the solvent molecules. CT states generally give rise to a broad-band emission, and the change of $\nu(t)$ with time is equated to either the peak frequency ($\nu_p(t)$) or the first moment of the emission band ($\bar{\nu}(t)$).[107]

Transient absorption and fluorescence up-conversion methods are most commonly used for the measurement of $\nu_p(t)$ or $\bar{\nu}(t)$. As already noted in section 2, for fluorescent molecules, whenever possible, the up-conversion technique is advantageous. As regards the chromophores, a suitable probe for the measurement of $C_\nu(t)$ should fulfill certain requirements. First, one has to verify that the observed dynamics is solely due to solvation; other possibilities, such as twisting or intramolecular vibrational relaxation, should not come into play. Furthermore, the chromophore must be chemically inert; that is, specific chemical interactions between the solute and solvent molecules should be absent. Finally, the chromophore should preferably exhibit a large Stokes shift so that the temporal dependence of $\nu(t)$ can be followed over a wide frequency range. This is the reason chromophores with an appreciable dipole moment in the excited CT state have been extensively used as probes in solvation studies. We now consider typical examples of such chromophores.

3.1.2. Styryl Dyes

A. DCM. DCM (4-(dicyanomethylene)-2-methyl-6-(*p*-(dimethylamino)styryl)-4*H*-pyran; for structure, see Figure 3) is well-known as a very efficient laser dye in the red.[1,2,108−113] In solution, DCM exists mainly in the trans isomeric form, the trans → cis isomerization barrier in the molecular ground state being high enough to prevent thermal isomerization to the cis form.[111−115] The optical spectrum of DCM consists of a broad band absorption and a strong broad band emission (with maximum band intensities near 465 and 630 nm, respectively, when the solvent is methanol (Figure 3)).[113] The large Stokes shift, as characterized by the large separation between absorption and emission peaks (∼160 nm) and the small spectral overlap between the absorption and emission bands, is mainly due to the disparity in the dipole moments of the molecule in its ground (6.1 D) and emissive excited state (26.3 D).[113] The large dipole moment in the emissive excited state characterizes this state as a CT state (the dimethylamino moiety acts as the electron donor and the two-cyano pyran moiety as the electron acceptor). In polar solvents, the CT state is favored and no emission from the locally excited (LE) state is observed.[108−110] The lifetime is ∼2 ns (2.2 ns in dimethyl sulfoxide (DMSO); 1.4 ns in methanol);[110] the quantum yield of the fluorescence is high (∼80% in DMSO; ∼40% in methanol).

Picosecond transient behavior of electronically excited DCM in polar solution was first found by means of time-resolved stimulated emission spectroscopy.[116] It was shown that, following the optical pump pulse, the stimulated emission signal is pro-

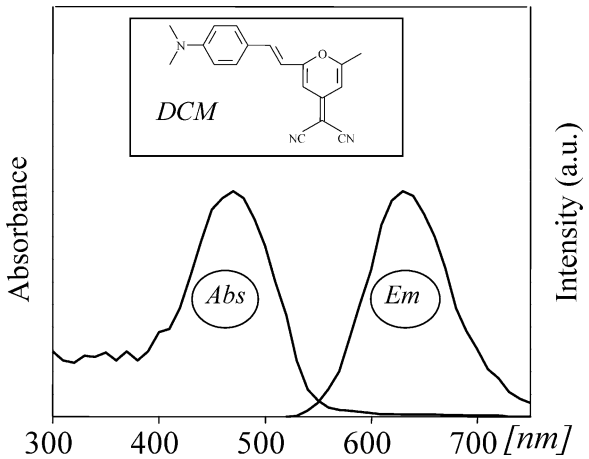

Figure 3. Steady-state absorption and fluorescence spectra of DCM dissolved in methanol. DCM structure is included as insert.

duced within 300 fs. The temporal behavior of the stimulated emission was investigated at various detection wavelengths. At shorter wavelengths, a picosecond decay is observed, whereas detection at the longer wavelengths yielded a picosecond rise component. The picosecond results appeared compatible with a picosecond red shift of the stimulated emission band. The kinetic behavior was unlike that for the dual band emission observed for 4-*N*,*N*-dimethylaminobenzonitrile (DMABN), where the feeding of the "red" band is at the expense of the "blue" band.[74,75] Since the pump−probe experiments for DCM did not show an isosbestic point in the temporal dependence of the stimulated emission spectrum in the investigated time window after ∼300 fs, a nonadiabatic LE-to-CT state transition (electron transfer) as in DMABN could be excluded, at least for $t >$ 300 fs.[116,117] The picosecond dynamic Stokes shift of the stimulated emission from DCM was attributed to solvation.[116,117] A plot of the empirical function, $C_\nu(t)$, yielded a single-exponential decay with a characteristic time of ∼3 ps for DCM in methanol and ∼8 ps in ethylene glycol. These times are compatible with the typical solvation times found for other probes in these solvents.[118]

Transient absorption/gain experiments for DCM in methanol with a much higher time resolution (∼40 fs) were performed by Ernsting et al.[119] An early transient spectrum was measured with a time constant of ∼140 fs. The spectrum was attributed to originate in the LE state, which was said to decay into the CT state. In agreement with the results of Easter and Baronavski,[116] the observed dynamics for $t >$ 300 fs was attributed to solvation in the CT state.[119] Martin et al.[120−122] have also performed transient absorption experiments for DCM dissolved in various polar solvents. In contrast with the results of Ernsting et al., a temporary isosbestic point was claimed to occur at 3−18 ps (instead of ∼140 fs) after the pump pulse. However, the time resolution (>0.5 ps) in the experiments of Martin et al. was an order of magnitude worse than that in refs 116 and 119, and this may be the reason for the discrepancy in the given LE- to-CT transition times. Recently, Maciejewski et al.[123] reported pump−probe experiments with ∼120 fs time resolution for DCM in cyclohexane and methanol. The emission of DCM in cyclohexane is due to the LE state, which is found to have a lifetime of 16 ps. The relaxation of the LE state of DCM in the nonpolar solvent is mainly to the S_0 ground state, although to a very small extent structural changes of DCM, possibly trans → cis isomerization, might also be present.[123,124]

Relaxation of electronically excited DCM has also been investigated by means of the femtosecond fluorescence up-conversion technique.[125−127] As already noted in section 2, the femtosecond fluorescence up-conversion method gives information about the temporal behavior of the population of only the emissive state, without the interference of ground-state bleaching, excited-state absorption, and stimulated emission. Figure 4 shows a few typical fluorescence up-conversion transients of DCM in ethylene glycol at different detection wavelengths.[125,126] The

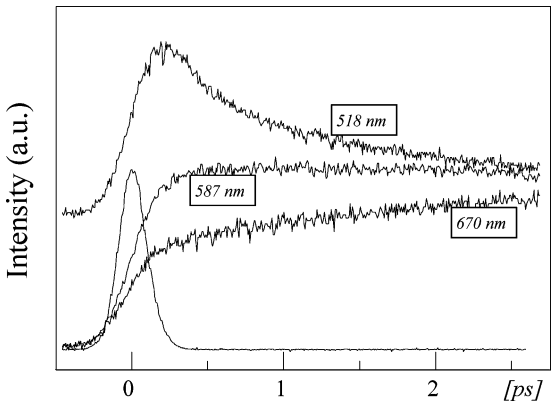

Figure 4. Typical fluorescence up-conversion transients observed for DCM dissolved in ethylene glycol at various wavelengths. Detection wavelengths are indicated.

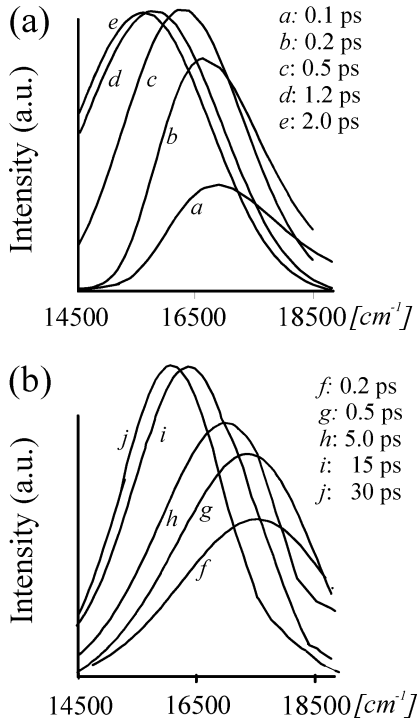

Figure 5. Time dependence of reconstructed fluorescence spectra of DCM dissolved in (a) acetonitrile and (b) ethylene glycol.

overall features are characteristic of a dynamic Stokes shift as also confirmed from a spectral reconstruction analysis.[69,125,126] Figure 5 shows the temporal variation of the reconstructed emission spectrum for DCM in the polar solvents acetonitrile and ethylene glycol (time resolution ≈ 100 fs).[126] The time dependence of the Stokes shift in various solvents is illustrated by the time dependence of the frequency of the peak of the emission band (Figure 6). Similar results for the dynamic Stokes shift were obtained in the up-conversion experiments of Gustavsson et al.[127]

The Stokes shifts of Figure 6 showed bimodal early time behavior (see inset in Figure 6). The solid curves in Figure 6 are best fits to a function of the form

$$C_\nu(t) = a_G \exp(-\omega_G{}^2 t^2/2) + \sum_{i=1}^{2} a_i \exp(-t/\tau_i) \quad (6)$$

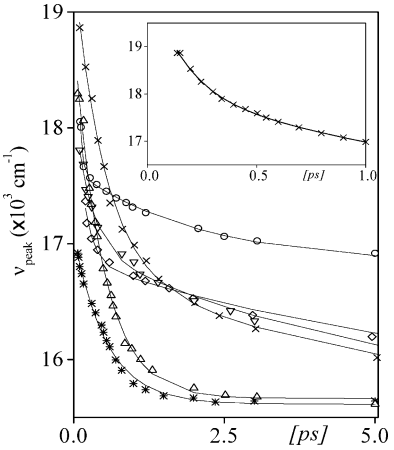

Figure 6. Time dependence of the fluorescence band maximum (in cm^{-1}) of DCM dissolved in methanol (×), ethylene glycol (◇), acetonitrile (∗), ethyl acetate (○), mixture of methanol/ethylene glycol (▽), and mixture of methanol/acetonitrile (△). The solid curves are the best fits to eq 6.

Table 1. Fitting Parameters of Solvent Correlation Function, $C_\nu(t)$,[a] of the Functional Form $C_\nu(t) = a_G \exp(-\omega_G^2 t^2/2) + \sum a_i \exp(-t/\tau_i)$, as Determined from Dynamic Stokes Shifts of DCM Dissolved in the Solvents Indicated[126]

solvent	a_G	ω_G (ps^{-1})	a_1	τ_1 (ps)	a_2	τ_2 (ps)	total shift[b] (cm^{-1})	τ_e[c] (ps)
methanol	0.2	6	0.5	0.7	0.3	5	3800	1
ethylene glycol	0.3	13	0.4	3	0.3	27	2400	4
acetonitrile[d]			1.0	0.5			1400	0.5
ethyl acetate	0.4	7	0.6	2			1400	0.9

[a] $C_\nu(t)$ is defined as given in eq 5. [b] The total shift is calculated by adding the preexponential factors obtained by fitting the *unnormalized* peak position $\nu_p(t) - \nu_p(\infty)$, instead of the *normalized* $C_\nu(t)$, to a function of the same form; $\nu_p(\infty)$ is obtained from the steady-state fluorescence spectrum. [c] τ_e is the time required for $C_\nu(t)$ to decay to $e^{-1} = 0.368$; it represents an average solvation time. [d] The solvation dynamics of acetonitrile could not be fitted with a Gaussian component. Presumably, the Gaussian component is too fast to be detected experimentally, and only the (exponential) trailing edge of the solvation is observed.

The parameter values used for the fits of Figure 6 are collected in Table 1.[126] The ultrafast decay components in the solvation process with a time constant of $1.4\omega_G^{-1}$ of about 100 fs are compatible with the short relaxation components reported for the probe molecules 1-aminonaphthalene, coumarin 153 (ref 128), and the styryl dye DASPI[129] (see also below) in polar solvents. Molecular dynamics and Brownian oscillator model calculations have shown that the fastest decay components in the spectral response function can be attributed to "inertial free streaming" motions of the small solvent molecules.[128−134] Small angle displacements are sufficient to account for about 30−40% of the total solvation dynamics.[126] The slower decay components of Table 1, on a time scale of a few picoseconds, compare with those found for other probe molecules in the same solvents[65−67,69−72,118] and are attributed to rotational diffusion motions of the solvent molecules.

Interestingly, concomitant with the dynamic Stokes shift, a rapid initial increase in the integrated emission intensity and an overall narrowing of the emission band (within 300 fs) could be discerned.[125,126] Simulations using a modified Smoluchowski diffusion equation approach[126] gave support to the idea that feeding of the CT state in DCM occurs from a higher lying state in approximately 300 fs. A similar conclusion was obtained recently from time-resolved stimulated Raman experiments.[135] A possible clue as to the nature of this "feeding" state are the aforementioned results of Kovalenko et al.[119] who concluded from their transient absorption experiments the existence of a LE state with a characteristic time of 140 fs. Our simulation results could be improved by assuming anharmonicity in the adopted potential energy functions; especially better agreement for the time dependence of the width of the DCM emission band with the experimental data could be obtained.[136] Very recently, similar nonlinear effects were considered to account for changes in the steady-state absorption and emission band shapes that accompany solvatochromic shifts of DCM[137] (and also of coumarin 153).[138−140] The nonlinear effects (which basically reflect the polarizability of the solute molecule in the excited state) were considered to arise from the combined effect of coupling between the LE and CT states on one hand and solvation on the other hand.

A dramatic slowing of the solvation relaxation process of DCM was observed for DCM in aerosol-OT (AOT) microemulsions in *n*-heptane.[141] In these microemulsions, the DCM molecules reside inside small water pools. In water pools, a dynamic Stokes shift of the fluorescence from the CT state markedly slower than that in the bulk of small polar solvents was observed; the discerned spectral response function for DCM was found to show a bimodal time dependence with charactersistic times of 280 and 2400 ps, respectively. Although due to the limited time response (∼50 ps) of the experiments ultrafast (subpicosecond) solvation dynamics might have been missed, these times are 2−3 orders of magnitude slower than those for the solvation dynamics in the bulk of polar solvents such as methanol or dimethyl sulfoxide (DMSO), but they are rightly predicted from simple continuum theory considering a slow Debye relaxation time of $\tau_D = 10$ ns for the water pool.[141,142] In addition, the time dependence of the emissive state of DCM was studied for the dye in micelles.[143,144] Now, in addition to the aforementioned slow solvation components that seem characteristic for organized microenvironments such as microemulsions[141] and aqueous protein solution,[145] an ultrafast solvation component of only a few picoseconds is observed. It was suggested that the results are representative of solvation of DCM at the micellar interface. Recently, solvation of DCM inside a nanocavity of another organized medium, namely, an aggregate of a bile salt, sodium deoxycholate in aqueous solution, has been studied.[146] A very slow solvation time with an average value of 1.9 ns was observed and attributed to DCM subjected to the slow motions of water molecules in the vicinity of the bile salt aggregate. It is noteworthy that unconventional solvation dynamics in an organized confined environment is currently attracting much theoretical and experimental interest.[147−150] The extension of the solvation

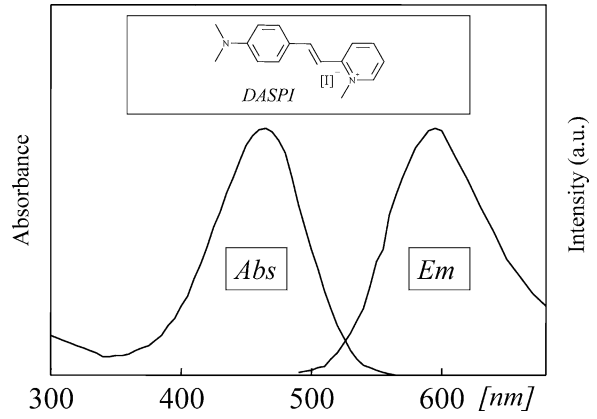

Figure 7. Steady-state absorption and fluorescence spectra of DASPI dissolved in methanol. DASPI structure is included as insert.

response to slower time scales has been related to the effects of the relatively slow (rotational and translational) dynamics of solvent molecules bound to the surface of the organized assembly/biomolecules; these solvent molecules are in dynamic equilibrium with quasi-free and bulk solvent molecules. The topic has been recently reviewed in a few excellent papers and is not considered further here.[147,148]

In summary, for DCM in polar solution, emission is from a charge transfer state that is populated within a few hundred femtoseconds following the laser-pulsed excitation of the locally excited (LE) state. Fast transient behavior of the fluorescence from the charge transfer state in small polar solvents is attributed to the effects of solvation. The solvation-induced fluorescence transients contain inertial free streaming (~100 fs) and rotational diffusion (approximately a few picoseconds) components. No indication of fast excited-state trans−cis isomerization (twisting) dynamics of DCM in polar solvents was found. In an organized confined environment like microemulsion, aqueous protein solution, or nanocavity, a dramatic slowing by orders of magnitude of the solvation process is measured. This topic is currently attracting much theoretical and experimental interest.[147,148]

B. DASPI. The polar styryl dye DASPI {2-(*p*-dimethylaminostyryl)pyridylmethyl iodide; for structure, see inset of Figure 7} shows an appreciable Stokes shift as illustrated by the positions of the band maxima in the absorption and emission spectra in methanol at about 460 and 635 nm, respectively.[151] Transient absorption and stimulated emission spectra for DASPI dissolved in methanol and acetonitrile were reported by Bingemann and Ernsting.[129] In these experiments, the time resolution after deconvolution was about 50 fs. From the results, the time dependence of the first, second, and third moments (typical of the mean frequency, width, and asymmetry) of the $S_1 \rightarrow S_0$ transition was determined. For DASPI in methanol, the time dependence of the mean frequency is given by a three-exponential decay function with characteristic times of 70 fs (30%), 800 fs (30%), and 6.4 ps (40%). The results are best understood by assuming that the frequency shift is caused by solvation. A fit for the solvation response was obtained with a three-mode Debye continuum approach.[65,129] Principally this approach does not include inertial motions of the solvent molecules to contribute to the solvation process. A better description of the time dependence of the emission band mean frequency for DASPI in acetonitrile was obtained starting from a multimode Brownian oscillator model, which considers a linear coupling of the electronic levels of the optically active probe to solvent modes that follow Langevin's equation of motion.[152] The best-fit parameters are $\nu_c = 22\ cm^{-1}$ and $\beta = 16\ ps^{-1}$ (ref 129), where ν_c and β refer to the frequency at the maximum of the spectral density of the liquid modes and the damping coefficient, respectively.[134]

The excited-state dynamics of DASPI was also investigated by means of the fluorescence up-conversion technique.[151] Fluorescence up-conversion transients for DASPI dissolved in methanol at different detection wavelengths similar to those of DCM (Figure 4) were measured. As in the case of DCM, after spectral reconstruction, the time dependence of the emission spectrum was obtained revealing a solvatochromic dynamic red shift. The time dependence of the peak frequency could be fitted to the functional form given in eq 6. This bimodal function indicates that the Stokes shift is due to the combined influence of inertial free streaming motions of the solvent molecules (Gaussian term) and a multiple-Debye term characteristic of rotational diffusion motions (exponential terms).[133,153] In Table 2, the fit parameters obtained for the solvation kinetics of DASPI in the solvents indicated are reproduced.[151] It is noted that a similar Gaussian decay component with $\omega_G = 6.0-12.0\ ps^{-1}$ (30−40%) has been found for the solvation of probe molecules such as coumarin 152,[72] coumarin 153,[118] and DCM.[116,125−127] This shows that different solute molecules show similar solvation behavior and that their solvation dynamics is not determined by solute specific solute−solvent interactions. The fast transients in the DASPI emission were absent in apolar solvents thus indicating that isomerization or twisting dynamics is not involved. In conclusion, DASPI and DCM show similar femto- and picosecond transient fluorescence behavior; the phenomena are attributed to the fast reorientational (inertial and rotational diffusion) response of the polar solvent molecules to the large dipole moment of the excited charge transfer state of the solute molecules.

C. DPD (Dimethylaminostyryl Pyridinium Dyes). Recently (sub)picosecond fluorescence studies have been extended to unbridged and bridged diphenyl derivatives of 1- or 4-(4′-dimethylaminostyryl) pyridinium dyes **1**−**4** (Figure 8).[154] These dye molecules have interesting applications as spectral sensitizers,[155] laser dyes,[156] and biosensors.[157] One of the motivations for a comparative study of these compounds was to establish whether bridging influences the presence of fast transients in the fluorescence. If so, one could argue that at least in part the excited-state dynamics is due to intramolecular functional group (twisting) motions, and one could question whether the fast transients are completely deter-

Table 2. Fitting Parameters of Solvent Correlation Function, $C_v(t)$,[a] of the Functional Form $C_v(t) = a_G \exp(-\omega_G^2 t^2/2) + \sum a_i \exp(-t/\tau_i)$, as Determined from Dynamic Stokes Shifts of DASPI Dissolved in the Solvents Indicated[151]

solvent	a_G	ω_G (ps^{-1})	a_1	τ_1 (ps)	a_2	τ_2 (ps)	$\Delta\nu^b$ (cm^{-1})	$\tau_e{}^c$ (ps)
methanol	0.14	6.0 ± 1.0	0.75	1.3 ± 0.5	0.11	12.4 ± 1.0	3500	1.0 ± 0.5
ethylene glycol	0.19	3.6 ± 1.0	0.38	2.8 ± 0.5	0.43	17.5 ± 1.0	3300	5.0 ± 1.0
ethanol	0.23	9.8 ± 1.0	0.32	1.0 ± 0.5	0.45	11.9 ± 1.0	2800	4.0 ± 1.0
acetonitrile	0.53	11.0 ± 1.0	0.47	0.8 ± 0.1			2000	0.3 ± 0.2

[a] $C_v(t)$ is defined as given in eq 5. [b] The total shift is calculated by adding the preexponential factors. [c] τ_e is the time required for $C_v(t)$ to decay to e^{-1}; it represents an average solvation time.

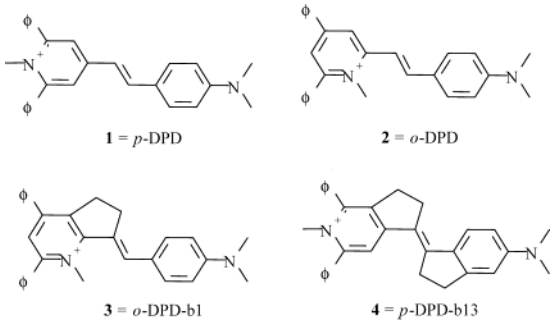

Figure 8. Structures of unbridged and bridged diphenyl derivatives of 1- or 4-(4′-dimethylaminostyryl) pyridinium dyes (DPD) **1**−**4**.

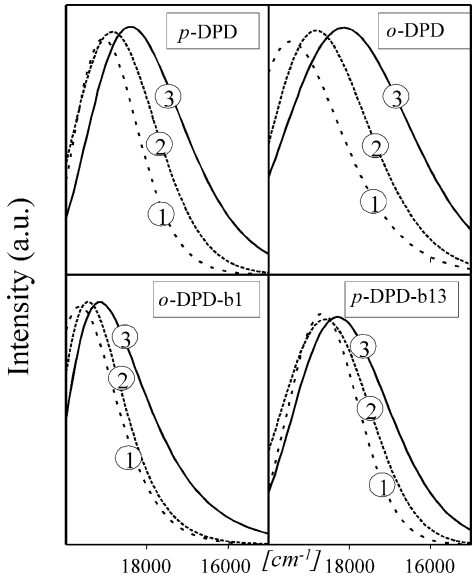

Figure 9. Steady-state fluorescence spectra of the DPD compounds **1**−**4** dissolved in (1) ethanol, (2) decanol, and (3) benzonitrile.

mined by solvation dynamics. The emissive state of the ionic styryl dyes **1**−**4** of Figure 8 is a charge transfer state in which charge has been transferred from the styryl group to the pyridinium acceptor.[5] In polar solvents, Stokes shifts typical of the charge transfer state of about 5000 cm^{-1} have been measured.[158] Figure 9 presents steady-state emission spectra of the DPD compounds **1**−**4** dissolved in ethanol, decanol, and benzonitrile. The spectra consist of a broad-band emission (maximum near 660 nm, fwhm about 2500 cm^{-1}); in the highly polar solvent benzonitrile, the DPD cation emissions are red-shifted compared to the emissions from the ethanol and decanol solutions, as expected for emission from a charge transfer state. Time-resolved fluorescence up-conversion transients and time-correlated single-photon counting experiments were

Table 3. Excited-State Lifetimes (in ps) for Ionic (4′-Dimethylaminostyryl) Pyridinium Dyes (1−4 of Figure 8) in the Solvents Indicated[154]

	ethanol	benzonitrile	decanol
p-DPD	80	215	900
o-DPD	40	85	400
o-DPD-b1	65	230	500
p-DPD-b13	1400	2000	2400

performed for the DPD compounds in ethanol, benzonitrile, and decanol.[154] As for DCM and DASPI, the fluorescence showed fast transient behavior that is detection wavelength dependent. From the time dependence of the emission spectra obtained after spectral reconstruction a dynamic Stokes shift of the emission band maximum was concluded.[154] The results show that for *p*-DPD in ethanol the dynamic Stokes shift (DSS) is approximately 1600 cm^{-1} in about 20 ps, in benzonitrile the DSS is about 1000 cm^{-1} in less than 10 ps, and in decanol the DSS is about 1600 cm^{-1} in more than 500 ps. The excited-state population decay to the ground state is much slower than the dynamic Stokes shift. The variation of the lifetime of *p*-DPD in the three solvents is given in Table 3.[154] Analogous dynamic Stokes shifts were obtained from the fluorescence transients measured for **2** (*o*-DPD), **3** (*o*-DPD-b1), and the double-bridged compound **4** (*p*-DPD-b13). This is reflected in the temporal dependence of the first moment of the emission bands of **1**−**4** as shown in Figure 10. An interesting result of the DSS measurements is that bridging of *both* single bonds of the styryl dye has no significant influence on the rate of the dynamic Stokes shift (e.g., compare spectral dynamics of **1** and **4** in Figure 10). This result is a strong indication that the rate of the Stokes shift of styryl dyes is *not* determined by twisting about a single styryl bond. Alternatively, since for the ionic styryl dyes **1**−**4** it is observed that the Stokes shift dynamics varies with the nature of the solvent and considering also that the probed molecules are chemically inert with respect to the solvents ethanol, benzonitrile, and decanol, it is very likely that the observed dynamic Stokes shift is due to solvation. Hence, according to the classification of section 1, the ionic styryl dyes **1**−**4** show fast excited-state dynamics predominantly due to solvation. The time dependences of the first moment of the emission bands of **1**−**4** are in agreement with this interpretation. The time constants and relative amplitudes characterizing the biexponential time dependences are given in Table 4. The table includes the average solvation times as known for the different polar solvents used here.[118] The weighted average times for the dynamic Stokes shifts of the styryl dye emission bands as discerned from

Table 4. Characteristic Times, τ_i (in ps), of the Biexponential Fit of the Dynamic Stokes Shift of the Emission Bands of the (4′-Dimethylaminostyryl) Pyridinium Dyes in the Solvents Indicated[154] [a]

	ethanol			benzonitrile			decanol		
	τ_1	τ_2	τ_{av}[b]	τ_1	τ_2	τ_{av}[b]	τ_1	τ_2	τ_{av}[b]
p-DPD	0.2 (0.3)	10 (0.7)	7.1	0.8 (0.4)	19 (0.6)	11.7	53 (0.3)	330 (0.7)	233
o-DPD	3.5 (0.7)	19 (0.3)	8.2				45 (0.6)	460 (0.4)	211
o-DPD-b1	1.9 (0.6)	24 (0.4)	10.7				45 (0.4)	210 (0.6)	136
p-DPD-b13	1.8 (0.8)	5.8 (0.2)	2.6	9.5 (0.5)	17.7 (0.5)	13.6	82 (0.5)	550 (0.5)	339
τ_{av}[118] [c]			16			5.1			245

[a] Relative amplitudes, defined as $a_i/(a_1 + a_2)$, where a_i is the amplitude of the ith component in the biexponential fit, are given in parentheses. [b] The average solvation time is defined as $\tau_{av} = (a_1\tau_1 + a_2\tau_2)/(a_1 + a_2)$. [c] The values of τ_{av}[118] are the characteristic times taken from Table 3 of ref 118.

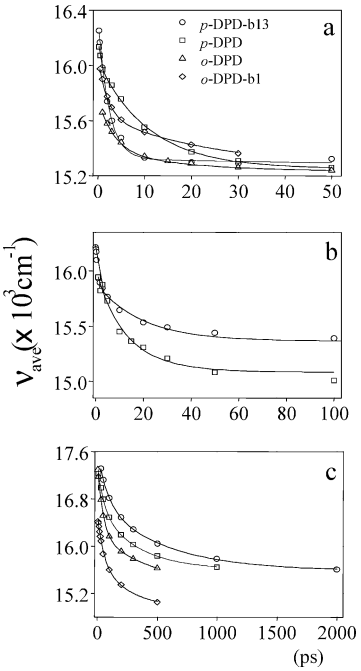

Figure 10. Time dependence of the first moment of the fluorescence band of DPD compounds **1**−**4** dissolved in (a) ethanol, (b) decanol, and (c) benzonitrile.

experiment and the known average solvation times of the solvents compare to within a factor of about three. This strongly suggests that the dynamic Stokes shift is mainly due to solvation dynamics in the excited state.

As seen from Table 3, if the styryl dye has at least one unbridged single bond adjacent to the styryl-group double bond (compounds **1**−**3**), the lifetimes of the corresponding compounds in a given solvent are comparable. If, however, both single bonds are bridged, like in **4**, the excited-state lifetime is lengthened significantly (by a factor of at least 10 when the solvent is ethanol). It is likely that the enhanced nonradiative decay of compounds **1**−**3** is related to the flexibility (torsional or bending) of functional groups that are linked by a single bond to the remainder of the molecule. The presence of single-bonded flexible groups can thus be viewed to lead to increased coupling of the excited state to the dense manifold of vibrational levels of the ground state thus facilitating effective radiationless decay. The flexible-group motions also depend on the viscosity of the solvent. As the viscosity of the solvent increases, the torsional or bending motions slow, and this will reduce the rate of the radiationless decay process.

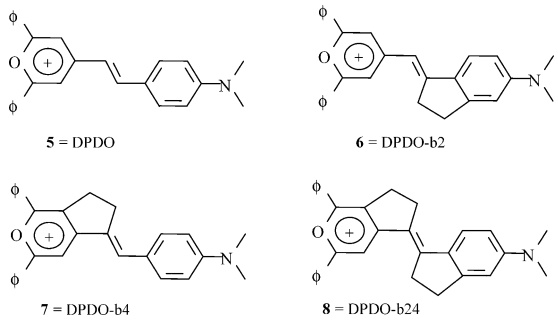

Figure 11. Structures of DPDO styryl dyes **5**−**8**.

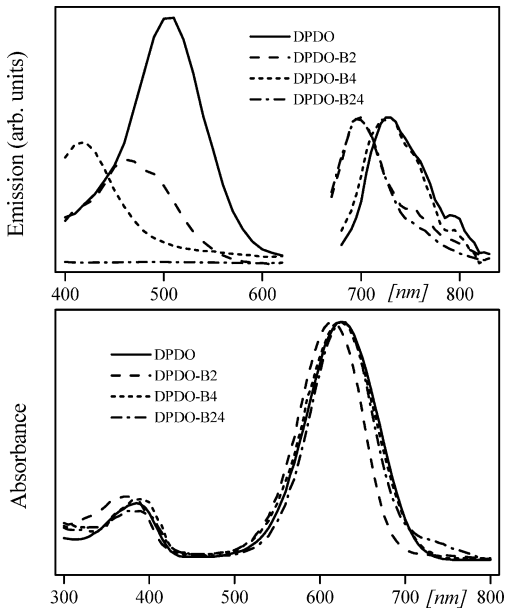

Figure 12. Steady-state absorption and fluorescence spectra of the DPDO compounds **5**−**8** dissolved in acetonitrile.

This is indeed verified from the change of the excited-state lifetime of each of the styryl dyes with the viscosity of the solvent: in higher viscous solutions, longer lifetimes are found.

For completeness, we mention also some preliminary femtosecond fluorescence up-conversion results for ionic styryl DPDO dyes **5**−**8** depicted in Figure 11.[159] These compounds contain a pyrylium group instead of a pyridinium group as in the DPD compounds of the previous section (nitrogen atom in the pyridinium group is replaced by oxygen). As shown in Figure 12, the absorption spectrum of the DPDO compounds consists of a main absorption band peaking near 620 nm and a much weaker band with a

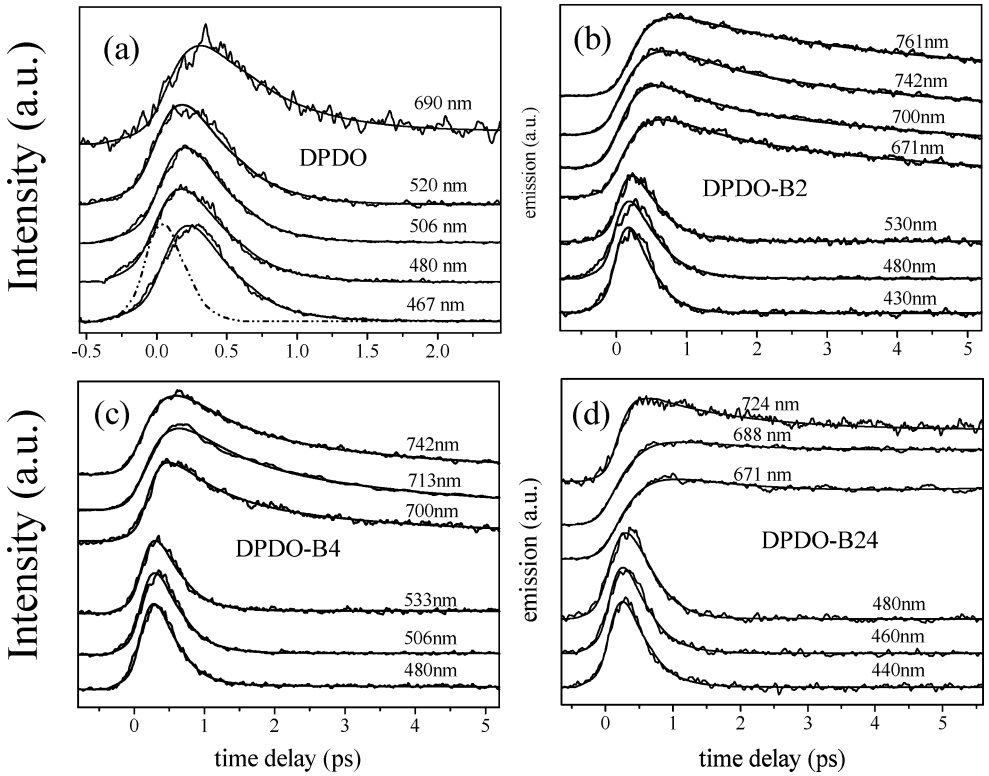

Figure 13. Fluorescence up-conversion transients of DPDO compounds **5**−**8** dissolved in acetonitrile. Detection wavelengths (in nm) are indicated. Solid curves are best fit to a multiexponential function convoluted with the instrumental response function (dash−dotted line).

peak near 385 nm. The emission spectrum shows two bands (Figure 12) with maximum intensities near 730 nm (not including the weak shoulders on the red side of the emission band) and 450 nm. It appeared that the two-band emission, not reported for the DPD molecules,[5,154] can be assigned as emissions from the S_2 state and the S_1 state, respectively.[159] Figure 13 shows a few fluorescence up-conversion transients monitored for **5**−**8** in acetonitrile.[159] The "blue" emission transients show an almost instantaneous rise followed by a decay with a time constant of ∼250 fs. The "red" emission of the DPDO compounds shows a ∼250 fs rise, followed by a biexponential decay with typical times of a few hundred femtoseconds and a few picoseconds. The similar time constants for the decay and rise of the blue and red emissions, respectively, shows that the depletion of the higher emissive state and the feeding of the lower emissive state occur concurrently. The 450 nm emission is attributed to the $S_2 \rightarrow S_0$ transition and the 700 nm emission to the $S_1 \rightarrow S_0$ transition.[159] The ∼250 fs process thus involves the $S_2 \rightarrow S_1$ internal conversion. The internal conversion time shows some variation with the solvent: ∼300 fs in methanol; ∼400 fs in ethanol; ∼700 fs in benzonitrile. These times are comparable to internal conversion times of 450−600 fs reported for all-*trans*-1,8-diphenyl-1,3,5,7-octatetraene and 1,6-diphenyl-1,3,5-hexatriene, respectively.[160,161] The measured rise times of the S_2 state are very close to known characteristic solvation times in methanol, ethanol, and benzonitrile (210, 290, and 850 fs, respectively[118]). This suggests that, although solvation dynamics may be obscured (due to concurrent internal conversion) in the fluorescence from the S_1 state, it is still possible to observe solvation dynamics for the DPDO probe molecules in the time dependence of the blue-band emission from the S_2 state. Solvation dynamics studies after selective excitation of the S_1 state of the DPDO dyes is not possible because the detection wavelength of the up-conversion signal is too close to the wavelength of the excitation pulse, and hence, due to this spectral overlap the up-conversion method cannot be used.

Since similar $S_2 \rightarrow S_1$ internal conversion kinetics is found for **5**−**8**, bridging apparently does not influence internal conversion. On the other hand, bridging does affect the lifetime of the excited S_1 state. For **5**, **6**, and **7**, the lifetime of the S_1 state is measured to be between 1 and 30 ps (depending on the solvent), whereas for **8**, the lifetime of the S_1 state is found as 0.61 ns in methanol and 1.98 ns in benzonitrile.[159] As found for the DPD compounds of the previous section, when twisting about single bonds is not possible, excited-state relaxation of the totally bridged styryl cation is slowed appreciably. Apparently, twisting motions about single bonds provide for effective nonradiative decay of the S_1 state to the ground state.

D. LDS-750 LDS-750 {6,7-benzo,3-ethyl,2-[1′,3′-butadienyl,4′-(4″-dimethylaminophenyl)] benzothiazolium perchlorate; for structure, see Figure 14} was the first styryl dye used in ultrafast time-resolved studies of solvation dynamics.[65,153] Like for other large-sized laser dye molecules in polar solution, broad featureless steady-state absorption and emission bands are measured (with the absorption-band peak near 570 nm and an emission-band peak near 725 nm, when the solvent is DMSO).[64] Femtosecond fluorescence up-conversion experiments have been performed for the dye molecule dissolved in aceto-

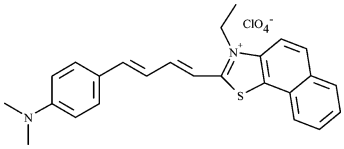

Figure 14. Structure of 6,7-benzo,3-ethyl,2-[1′,3′-butadienyl,4′-(4″-dimethylaminophenyl)] benzothiazolium perchlorate (LDS-750).

nitrile.[69,153] After spectral reconstruction, fluorescence spectra at various times were simulated and a very fast dynamic Stokes shift of the emission band maximum to the red was revealed. In acetonitrile, the dye gives rise to a solvatochromic shift of about 50 nm, ~80% of which occurs within ~150 fs.[153] This dynamic shift is absent in frozen acetonitrile indicating that the dynamics in the liquid is due to solvation and that intramolecular vibrational relaxation is not important in the ultrafast relaxation process. The initially Gaussian-shaped solvation response function (for $t \leq 100$ fs) was discussed to originate from small amplitude inertial rotational motions of the aprotic solvent molecules, whereas the slower second part of the solvent response (0.5−1 ps) was assigned to diffusive motions of the solvent molecules. The proposal that the ultrafast initial relaxation derives from solvation was contested by Kovalenko et al.[162] By means of the pump/supercontinuum probe (PSCP) technique (~40 fs time resolution), transient absorption and gain spectra were monitored in a time range up to about 1 ps. In acetonitrile, at relatively low pump energy (0.3 μJ), an intermediate excited electronic state was proposed to be populated initially (within 70−140 fs), followed by a second step in which the intermediate state decays into the final state, which is reponsible for the gain spectrum. The overall time of ~200 fs for these processes was assumed to involve a two-step isomerization of LDS-750. On the other hand, the measured rate of the conformational changes is still influenced by the solvent polarity, so the excited-state dynamics was largely but not completely assigned to intramolecular isomerization.[162]

Recently, Yoshihara and co-workers performed femtosecond time-resolved fluorescence experiments of LDS-750 in aniline.[163] A dynamic Stokes shift to lower energy for the emission was observed. The deduced spectral shift correlation function, $C_\nu(t)$, could be modeled satisfactorily using the dynamical mean spherical approximation (DMSA)[66,118] and the pure liquid data. It was concluded that the fluorescence dynamics is determined by solvation only. Furthermore, the ultrafast initial decay of $C_\nu(t)$ of LDS-750 in aniline, with a typical time of ~300 fs (25%), was found to be compatible with the results of Bingemann and Ernsting[129] for LDS-750 in other solvents and to correlate with the changes expected for the inertial frequency of the solvent molecular motions. The results did not agree with the predicted influence of the solvent viscosity on intramolecular conformational motions. The time-resolved fluorescence spectra also show a broadening by 40% over the first 20 ps. It was proposed that this broadening is representative of conformational changes of the styryl dye that accompany the solvation process. Possibly the conformation of the solute and the configuration of the surrounding solvent molecules are coupled and thus may influence each other.[163]

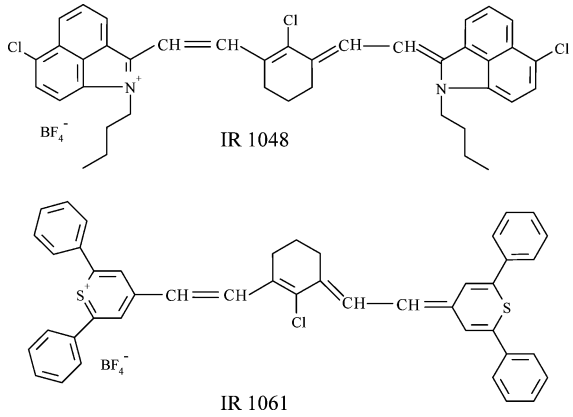

Figure 15. Structures of chromophores IR 1048 and IR 1061.

Table 5. Fitting Parameters for Fluorescence Transients of IR 1048 and IR 1061 in Acetonitrile (acn), Dichloromethane (dcm), Ethanol (EtOH), and Hybrid Films[166,167] [a]

	τ_1 (ps)	A_1	τ_2 (ps)	A_2	$\eta \pm \Delta\eta$
			IR 1048		
EtOH	0.10	−0.08	6.7	0.07	0.001 ± 0.001
acn	0.13	−0.12	7.9	0.36	0.002 ± 0.001
dcm	0.31	−0.14	15.3	0.71	0.004 ± 0.001
film			15 ± 3	1	0.006 ± 0.001
			IR 1061		
EtOH	0.28	−0.16	17.9	0.52	0.005 ± 0.001
acn	0.12	−0.80	28.9	0.78	0.009 ± 0.003
dcm	0.18	−0.20	38.9	0.20	0.017 ± 0.005
film			25 ± 4	1	0.014 ± 0.005

[a] τ_i and A_i represent decay times and relative amplitudes, respectively. Detection wavelength is 1120 nm for the solutions. A single-exponential decay function has been employed to fit the transients of the films. The lifetimes in the film have been obtained by averaging over six measurements at different detection wavelengths. Quantum efficiencies are reported in the last column.

E. IR Dyes. Recently, ultrafast studies of chromophores that show luminescence in the infrared (IR)[164,165] have been performed.[166,167] As is well-known, the IR region is crucial for fiber optics communication. The structures of the cyanine dye IR 1048 and the thiopyrilium dye IR 1061 of these studies are sketched in Figure 15. Considering the structures of these IR dyes, it is not clear a priori whether the emission would contain fast components and, if so, what would be the nature of such behavior, solvation, configurational dynamics (perhaps due to flexible double bonds), or both. The spectra of the two dyes show an absorption band maximum near 1065 nm and a broad structureless emission peaking near 1075 and 1085 nm in a hybrid sol−gel film. Femtosecond fluorescence up-conversion transients could be measured. A fast time component, characterized by a time constant τ_1, is observed. This component shows an emission wavelength dependence: it appears as a decay when detection is in the blue part of the emission (1020−1040 nm) and as an increase (build-up) in the red part (1090−1150 nm), the time constants being similar. Table 5 includes τ_1 values for IR 1061and IR1048 in various solvents and in a

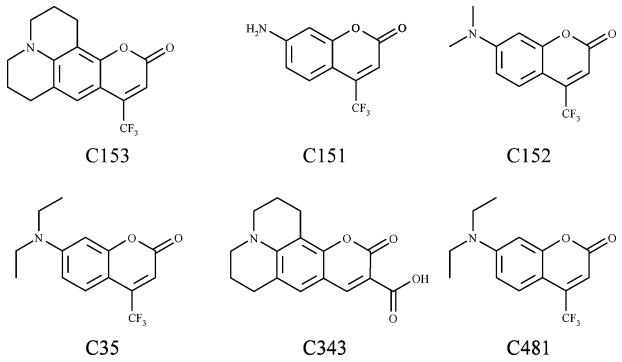

Figure 16. Structures of several coumarins.

thin hybrid sol−gel film, when detection is at 1120 nm. The τ_1 component depends slightly on the nature of the employed solvent and is absent when the solutes are doped in films. The subpicosecond τ_1 component was attributed to only solvation involving (short-range) interactions between the solute molecules and nearest-neighbor solvent molecules undergoing fast reorientational motions (which are damped in the film).[167] The characteristic time τ_2 is representative of the lifetime of the relaxed excited state. τ_2 appeared to be solvent-dependent: in acetonitrile the lifetime is shorter than that in dichloromethane. The even faster decay time in ethanol may hint to specific solute−solvent interactions.

3.1.3. Coumarins

A. Coumarin 153. Due to its rigid structure, strong radiative character, and simple solvatochromic behavior,[168−170] coumarin 153 (C153; for structure, see Figure 16) has been one of the most thoroughly investigated probes in studies of solvation dynamics. Maroncelli and Fleming[69] were the first to extensively examine fast components in the emission of C153 (lifetime ≈ 5 ns) in various solvents utilizing picosecond fluorescence spectroscopy. Although the time resolution of these early experiments was rather limited (∼30 ps), it was verified that the fluorescence of C153 shows a solvent- and polarity-dependent dynamic Stokes shift that could be attributed to solvation. The Stokes shift was rationalized on the basis of the excitation-induced change in the dipole moment of the solute from ∼5.6 (ground state) to ∼10−14 D (excited state). The time dependence of the spectral response function was found to be multiexponential, the more so in solvents with higher polarity, and therefore appeared inconsistent with the predictions from simple continuum theory.[95−97] It was suggested[69] that a large part of the solvation is determined by interactions between the solute and nearest-neighbor solvent molecules thus making bulk properties of the solvent, which are responsible for the longitudinal relaxation time in continuum theory, less relevant. Experiments with high time resolution (∼100 fs) revealed more details of the spectral response function of the system immediately after the optical excitation pulse.[118] Unlike earlier studies (with less time resolution),[72] the measurements of Horng et al.[118] showed the existence of bimodal decay behavior of the spectral response function with a fast decaying component in the (100−300 fs) region. The presence of this component was demonstrated regardless of whether C153 was dissolved in protic or aprotic polar solvent. The ultrafast decay was attributed to the contribution of inertial motions of the solvent molecules to the spectral response, in agreement with previous predictions.[70,171] Similar inertial component dynamics in polar solvents was found in later experiments with DCM as the solute (vide supra).[116,125] Vibrational relaxation could be excluded as a possible mechanism for the observed ultrafast relaxation component. This was concluded from the absence of any ultrafast shift component for C153 dissolved in cyclohexane in which C153 is unlikely to show solvation dynamics. Simulations suggested that vibrational relaxation would manifest itself in the fluorescence spectrum as a quickly disappearing blue part and a concomitantly rising red part. On the time scale of 100 fs or longer, no such phenomena were observed. On the contrary, already for $t \approx 100$ fs, the fluorescence spectrum assumes the shape of the steady-state emission spectrum (although to a percentage of about 10%, residual rise and decay components with times in the range of 1−10 ps were also found). It was concluded that intramolecular vibrational redistribution is much faster (≤30 fs) than the inertial motions of the solvent molecules and that the picosecond components are probably due to vibrational cooling, that is, dissipation of excess vibrational energy to the bath of solvent molecules.[118]

Transient absorption and gain spectra of C153 in acetonitrile and methanol were also measured with ∼40 fs time resolution using a pump/supercontinuum probe technique.[172] At the earliest times (t < 70 fs), the excited-state absorption and the stimulated emission spectra show vibrational structure. The novel feature was that the red shift of the stimulated emisssion is not accompanied by a synchronous blue shift of the excited-state absorption. It was inferred that, concomitantly with solvation dynamics, C153 undergoes a stepwise intramolecular excited-state electronic relaxation to two other excited singlet states, in agreement with earlier findings of Blanchard and co-workers from picosecond pump−probe experiments.[173,174] The multi-excited-state relaxation mechanism has been refuted by Maroncelli et al., however.[175] On the basis of their finding that there is no observable influence of the nature of the solvent on the absorption or the emission transition moment, they conclude that it is very unlikely that more than two electronic levels are involved in the optical cycle.

In a recent study by Gustavsson et al.,[176] the idea that the ultrafast decay component(s) in the fluorescence of C153 is completely due to solvation dynamics has been contested. After an elaborate deconvolution procedure of the time-resolved fluorescence upconversion spectra (from which they claim that the experimental time resolution becomes around 50 fs, the instrument response function being ∼220 fs), the authors find that more than 50% (instead of 30% reported by Maroncelli et al.) of the dynamic Stokes shift consists of an ultrafast component with a characteristic time faster than 50 fs. It was argued that this component cannot be fully attributed to solvation dynamics and for the larger part must be due to

ultrafast intramolecular dynamics. Since the controversy seems to be sensitively affected by the method of the numerical analysis, the problem concerning the physics involved in the full trajectory of the dynamic Stokes shift may still need further investigation.

Although the majority of the time-resolved Stokes shift studies of C153 have been performed for the solute in polar organic solvents (like simple alcohols and alkyl cyanides),[65−67,69−72] solvation of the dye has also been studied in nonideal binary mixtures of alcohols and water,[177] water and organized assembly in water,[147,178−180] inorganic molten salts at high temperature,[181−183] ionic liquids at room temperature,[184−186] and small polymer environment.[187] In general, in these systems the dynamic Stokes shifts are slower, if not much slower, than in the molecular solvents. For instance, for C153 in a mixture of 1-propanol ($0 < X_{PrOH} < 1$), it was concluded that C153 is preferentially solvated by the alcohol (C153 is almost insoluble in water) and, as the 1-propanol fraction is increased, the solvation dynamics slows to about 15 ps for $X_{PrOH} \approx 1$.[177] The results are indicative of specific solute−solvent interactions. For coumarin C480, similar very slow solvation dynamics has been observed when the dye is confined in a water pool inside vesicles. Then, a bimodal solvation with characteristic times of 0.6 and 11 ns was measured.[179] When C480 is confined in water inside micelles, the typical solvation time is 180−550 ps, that is, again orders of magnitude slower than that in bulk water.[180] In molten salts, like tetrabutylammonium hydrogen sulfate and tetradodecylammonium perchlorate, the solvation dynamics of C153 is also slow. In these liquids, solvation times of 40 and 220 ps and 200 and 2000 ps, respectively, have been reported.[181−183]

Recently, solvation dynamics of C153 has been studied in the ionic liquids [BMIM][BF_4] (1-butyl-3-methylimidazolium tetrafluoroborate) and [EMIM][BF_4] (1-ethyl-3-methylimidazolium tetrafluoroborate).[184−186] The viscous liquids are more polar than acetonitrile but less polar than methanol. The solvation dynamics of C153 in these liquids, as characterized by the spectral shift function, is found to be bimodal, the short component being 120−280 ps and the long component being 1.3−4.0 ns, that is, about 3 orders of magnitude slower than those in simple organic solvents. The "faster" initial component is attributed to the influence of motions of the relatively small anions (BF_4^-), while the "slower" component originates in the combined influence of the cations and anions. Finally, recent time-dependent fluorescence anisotropy experiments of C153 showed that the solute is useful in studies of preferential solvation in nonideal solvent mixtures.[188,189] In these studies of preferential solvation, special solute−solvent interactions are considered to discuss the relatively slow (subnanosecond to nanosecond) solvation dynamics, and in this respect these studies differ from those considered so far for inert solutes in bulk solvents. Special solvation effects as in nonideal solvent mixtures or at surfaces of proteins, micelles, vesicles, aggregates, etc. are not considered further in this paper, however.

In summary, following pulsed laser excitation of C153 in a solution of small polar molecules, ultrafast transient behavior of the fluorescence is observed. At early times ($t < 50$ fs), the nature of the processes that determine the fluorescence dynamics is still under debate, but it is likely of intramolecular origin. On a time scale of 100 fs or longer, the transients are due to solvation; initially inertial motions of nearby solvent molecules dominate (100−300 fs); subsequently the dynamics is determined by rotational diffusion motions of the solvent molecules. As is the case for the styryl dye compounds DCM and DASPI, in confined environments (micelles, polymer, mixed solvents) the solvation dynamics slows dramatically.

B. Other Coumarins. Whereas for C153, due to the rigid structure of the molecule, the observed ultrafast Stokes shifts could be attributed to solvation dynamics and vibrational relaxation, other coumarins, such as C151, C152, and C35 (Figure 16), may contain flexible functional groups that allow for intramolecular conformational dynamics, and thus solvatochromism dynamics may become complicated by additional internal dynamics.[72,176] We defer the topic of distinguishing between ultrafast internal relaxation and excited-state deactivation caused by very rapid motions of solvent molecules to section 3.2.

A coumarin that has a rigid structure similar to that of C153 is coumarin 343 (C343, Figure 16). C343 has been used by Levinger et al. in studies of solvation dynamics in reverse micelles, microemulsions, and vesicles.[190−193] Generally, it was confirmed that when the solute is dissolved in a pool of solvent molecules in a restricted environment, the ultrafast solvation dynamics that normally exists in bulk solvent is slower by orders of magnitude.

For coumarin 481 (C481, Figure 16), the dynamics of internal conversion (IC) from a higher lying S_n state to the emissive S_1 state in cyclohexane solution[194] was recently studied by means of the method of femtosecond fluorescence up-conversion. Typical rise times of 220−280 fs, measured at all fluorescence wavelengths (and comparable to those mentioned above for the DPDO compounds), were attributed to the IC process, intramolecular vibrational energy redistribution being a much faster process. After internal conversion, a narrowing of the fluorescence band was observed. The phenomenon was attributed to the effect of cooling of the vibrationally "hot" S_1 state. Dissipation of the approximately 3500 cm^{-1} excess excitation energy in the S_1 state to the bath of solvent molecules occurs on a time scale of 10 ps.

3.1.4. Organic Light-Emitting Diode (OLED) Dyes

Thin films of vapor-deposited metal chelates, such as aluminum(III)-8-hydroxyquinoline (Alq_3), have been successfully applied as organic light-emitting diodes (OLED).[195−199] Several studies concerning the mechanisms and the dynamics of charge injection, charge transport, and charge recombination of Alq_3 have been undertaken.[200−205] In liquid solution, photoinduced fluorescence of Alq_3 has also been observed.[195,206] The lowest electronic states derive from $\pi \rightarrow \pi^*$ excitations localized at one of the quinolino-

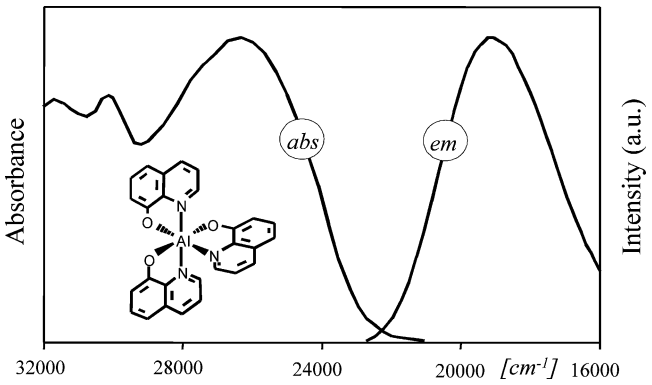

Figure 17. Steady-state absorption and emission spectra of Alq_3 dissolved in DMF. Structure of Alq_3 is given in insert.

late ligands with electronic charge being partially transferred from the phenoxide to the pyridyl side of the ligand.[197,204,205] The decay of the fluorescence is exponential with a typical lifetime of 10 ns at room temperature. Recently, time-resolved fluorescence studies of fast dynamics in Alq_3 and Gaq_3 have been performed.[207−209] For Alq_3, in solution, picosecond fluorescence transients were resolved by means of femtosecond fluorescence up-conversion and time-correlated single-photon-counting experiments.[207] Figure 17 shows the steady-state absorption and emission spectra of Alq_3 in DMF. Spectral analysis of the up-conversion transient results showed a dynamic Stokes shift of about 1000 cm^{-1} in a time between 300 fs and 10 ps; in this time, there is also a broadening of about 400 cm^{-1}. For Alq_3 doped in a $Al(acac)_3$ host crystal, *no* picosecond transients (i.e., no dynamic Stokes shift) could be observed. Moreover, the time constants for the short-time components in the fluorescence of Alq_3 in different solvents (DMF, DMSO, dichloromethane, and toluene) resemble those of the known solvent relaxation times for these solvents. Evidently, the picosecond components are due to solvation effects. It was also found that the solvation-induced dynamic Stokes shift is accompanied by a decrease of the integrated fluorescence intensity much faster than could be accounted for by the ν^3-law for spontaneous emission. To explain this intensity drop, it was conjectured that a solvent-induced mixing of close-lying excited molecular states takes place during the solvation process.[207]

Fluorescence transients measured for protonated 8-hydroxyquinoline in $HClO_4$ (not complexed to aluminum(III)) showed a time dependence very similar to that of the metal-chelated species; that is, spectral shifting occurs in time window from 300 fs up to 10 ps, and after spectral reconstruction the integrated intensity of the emission spectrum decreased much more rapidly than a ν^3 dependence.[207] In the N-protonated species 8-HHQ^+, the positively charged pyridyl moiety acts as a strong acceptor, and donor−acceptor transitions from the phenoxide donor are effectively enhanced. The large similarity in the kinetics of the fluorescence of the 8-HHQ^+ species on one hand and the Alq_3 complex on the other hand is support that, within the experimental time resolution of ∼100 fs, immediately following the laser pulse, the emissive state of the Alq_3 complex is localized on an individual ligand and that charge separation has taken place within the quinolinolate ligand in the excited state. Further support was obtained from time-resolved fluorescence depolarization experiments.[209] Again, the results obtained for the Alq_3 complex and the 8-HHQ^+ species were similar. Upon excitation with linearly polarized laser pulses, up-conversion transients for the emission polarized parallel ($I_{||}$) and perpendicular ($I_{\perp}$) to the polarization direction of the exciting laser pulses were measured. The time dependence of the fluorescence anisotropy, $r(t)$, was obtained from the best fit functions for $I_{||}(t)$ and $I_{\perp}(t)$. Fluorescence transients obtained for short excitation wavelengths (<326 nm) did not exhibit a temporal difference for $I_{||}(t)$ and $I_{\perp}(t)$. When excitation was near 360 nm, however, a nonzero value for $r(0)$ was found. The nonzero anisotropy implies that, within the system response time of 150 fs, the directions of the transition moments for absorption and emission remain, at least partially, correlated. A nonzero value for $r(0)$ rules out the possibility of an initial ultrafast excitation delocalization process involving the three quinolinate ligands. The values of 0.2 (detection at 505 nm) and 0.12 (detection at 600 nm) are lower than the theoretical limit of 0.4. This lowering is likely due to a diminished photoselectivity by the polarized excitation because of spectral overlap of several absorption bands (with different polarization) at the experimental excitation wavelengths (340−360 nm). Note that the partial directional correlation between the absorption and emission dipoles implies that internal conversion from the initial Franck−Condon state to the emissive state must be ultrafast and completed within the system response time of 150 fs. Such an ultrafast relaxation process was reported previously also for another metal complex, namely, $Ru(bpy)_3^{2+}$.[210] As remarked, $r(0)$ values of 0.2 and 0.12 were obtained when detection is at 505 and 600 nm, respectively. Since the final electronic state in the optical transition at these wavelengths is the same (namely, the electronic ground state), the different initial anisotropy values mean that the polarization of the emission of the initial states differs. A difference is understood on the basis of the above-mentioned ultrafast solvation mechanism. The "600 nm" emission is due to molecules that were populated by solvation while the exciting laser pulse is still "on" and that have a different mixing of the initial states than the molecules emitting at "505 nm". If the mixed states not only have different radiative character (leading to the intensity effects of solvation mentioned above) but also have different directions for the transition moment of the emission, then $r(0)$ is expected to vary with the detection wavelength.

The dynamics of the depolarization process, with a time constant of about 2.0 ps, compares very well with that of the dynamic Stokes shift and the solvent relaxation time of 1.7 ps of the solvent. Moreover, for Alq_3 doped in a host crystal or rigid glass, no fluorescence depolarization transients were observed. These results confirm that the 2.0 ps fluorescence anisotropy decay must be related to the solvation process. The absence of fast depolarization in rigid

medium also excludes that intramolecular relaxation like vibrational relaxation should be considered as a possibile cause for the picosecond behavior. On the other hand, normally solvation is not expected to influence the electronic transition dipole moment unless, as already mentioned above, during solvation the nature of the emissive electronic state is affected. This possibility was already raised above in the discussion of the magic angle results and is further supported by the results of the anisotropy experiments. The fluorescence anisotropy, $r(t)$, for Alq_3 in solution appeared to fit a biexponential function. Whereas the fast (~2 ps) component is related to the solvation process, the slow component is much longer (~85 ps for Alq_3 in DMF) and attributed to the rotational diffusion motions of the probed Alq_3 solute molecules. Several observations are in support of this interpretation. First, the "long" fluorescence anisotropy decay component is present only when the complexes are in liquid solution and becomes much longer as the solvent viscosity is increased (e.g., in ethylene glycol the decay time is 1.18 ns). Second, $r(t)$ appears to be independent of the detection wavelength, and finally, the "long" fluorescence anisotropy decay component slows when the atomic radius of the metal ion in Mq_3 is larger (i.e., the diffusional anisotropy decay is longer in the order Alq_3, Gaq_3 and Inq_3). In summary, femtosecond fluorescence up-conversion experiments have proved useful in verifying that in liquid solution the Alq_3 complex shows solvation dynamics that is also typical of the 8-HHQ^+ species. It is concluded that photoexcitation of Alq_3 leads (within ~100 fs) to a localized excitation at one of the quinolinolate ligands (no delocalized three-ligand excitation); this is further supported by results from femtosecond fluorescence anisotropy measurements.

3.2. Intramolecular Twisting Dynamics

3.2.1. Auramine

Whereas for the chromophores reviewed in the previous section the fastest components of the excited-state dynamics are predominantly due to the reorientational motions of the solvent molecules, we now turn to chromophores with transient excited-state behavior due to ultrafast intramolecular conformational changes. Such motions are of great importance to numerous processes in chemistry[64] and biology.[211] Very high values for the reaction rate (in excess of 10^{12} s^{-1}) may be obtained when the excited-state potential energy, as a function of the reaction coordinate, lacks an activation barrier. Solvent viscosity may then to a great extent still influence the excited-state dynamics. This has been extensively investigated for photoexcited di- and triphenylmethane dye molecules showing twisting dynamics of the phenyl groups.[212−216] Another example is the diphenyl-aminomethane dye cation auramine (Figure 18). Auramine is a yellow dye that is weakly fluorescent in low-viscosity solvents (e.g., water) and highly fluorescent in viscous solvents, DNA, and polymeric acids.[217,218] From early steady-state spectroscopic investigations, it was already concluded that diffusion-controlled twisting motions of the

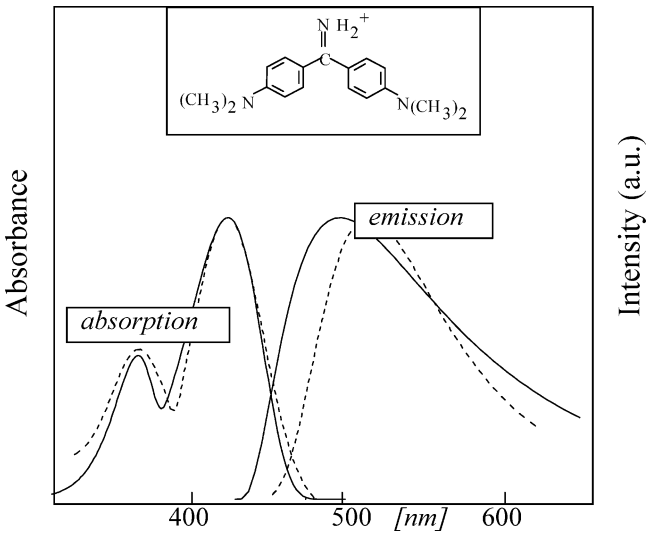

Figure 18. Steady-state absorption and emission spectra of auramine dissolved in ethanol (dashed curve) and decanol (solid curve). Structure of auramine is given as insert.

phenyl rings in the molecule play an important role in the relaxation of the locally excited state.[219] Recent time-resolved transient absorption and fluorescence up-conversion studies provided further information regarding the dynamics and mechanism of the excited-state relaxation process.[122,220−222] Figure 18 shows the steady-state absorption and emission spectra at room temperature of auramine dissolved in ethanol and decanol. The emission band maximum of auramine in ethanol is blue-shifted by about 800 cm^{-1} as the temperature is decreased from 293 to 173 K. Also, the total fluorescence intensity has increased by about a factor 5, in agreement with the quantum yield enhancements given in refs 219 and 223. Transient absorption measurements for auramine in ethanol showed the decay of a stimulated emission band (above 470 nm) in a few picoseconds after excitation and the simultaneous rise of a transient absorption near 480 nm, where the initial gain signal gives way to the new transient absorption band. A temporary isosbestic point is seen at 459 nm for a nonzero ΔD value indicating the presence of more than two species or excited states. At longer delays, both the induced absorption and bleaching bands decay.[220] In decanol, the transient spectra exhibit similar dominant features, but the kinetics are slower and more complex: a 10-ps lag prior to a single 130-ps exponential decay is found in the bleaching band.

Further evidence that several excited electronic states (and not just one state) are involved in the relaxation of the optical excitation in auramine was obtained from femtosecond fluorescence up-conversion experiments.[220−222] These experiments were performed for auramine in the solvents ethanol and decanol at room temperature. The influence of a change in the viscosity was examined for the auramine/ethanol solution by changing the temperature. Typical features observed in the fluorescence transients of auramine are illustrated in Figure 19. The figure shows fluorescence up-conversion transients for auramine dissolved in ethanol at three detection wavelengths (panel a) and three tempera-

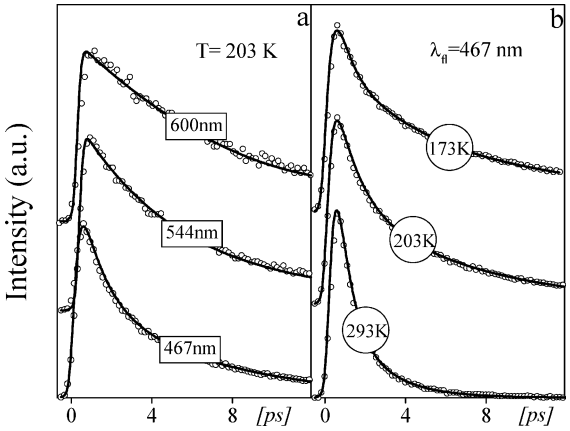

Figure 19. Typical fluorescence up-conversion transients of auramine dissolved in ethanol: (a) $T = 203$ K, detection wavelengths as indicated; (b) detection at 467 nm, temperatures as indicated.

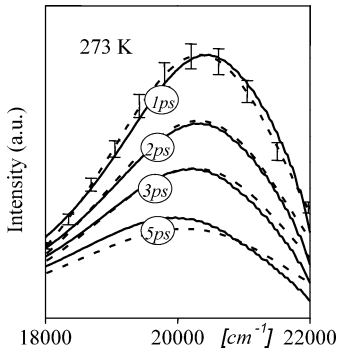

Figure 20. Simulated (solid) and experimental (dashed) time-resolved fluorescence spectra of auramine dissolved in ethanol. Excitation is at 480 nm.

tures (panel b). The time-dependent fluorescence spectra were obtained after spectral reconstruction.[220,221] Figure 20 shows as an example the temporal behavior of the emission band of auramine dissolved in ethanol at 273 K. A small dynamic Stokes shift of a few hundred wavenumbers (within the first 10 ps) accompanied by a drastic drop in fluorescence intensity to about 10% of the initial value is observed. The residual fluorescence has a longer decay of about 30 ps. This lifetime is thus the same as that of the 480 nm transient absorption. The transient absorption at 480 nm has been assigned as the absorption of a (quasi-) dark state.[122,220] From the similar time constants for the fluorescence decay and the rise of the transient absorption at 480 nm, it is concluded that the emissive locally excited (LE) state relaxes within about 2 ps into the weakly emissive excited state that, at room temperature, has a lifetime of 30 ps, which is labeled henceforth as S_{relax}. The rotational motions of the phenyl rings play an important role in the relaxation of the excited state of auramine. As the temperature is lowered, the viscosity increases and the torsional motions of the phenyl rings slow. This slowing affects the LE-to-S_{relax}-state relaxation, as manifested by the slower dynamic Stokes shift and the slower drop in the integrated emission intensity at lower temperatures. The effects could also be examined more quantitatively.[221] Two alternative models may be considered.

Bagchi et al.[224] considered the problem of a rapid drop in the integrated fluorescence intensity accompanying a barrierless reaction. The time development of an initial population distribution along an excited-state potential energy surface was simulated using a modified Smoluchowski diffusion equation containing a nonlocal sink function term that accounts for an enhanced nonradiative decay as the reaction proceeds. The kinetics of the fluorescence intensity decay and the dynamic Stokes shift will be similar if the rate of the nonradiative decay caused by the sink function term, on one hand, and the rate for population relaxation along the potential energy surface, on the other hand, are comparable. Albeit this is what is observed for auramine, the approach of Bagchi et al. still is not applicable in the case of auramine because the BFO model also implies that the typical lifetime of the relaxed excited state is eventually determined by the sink function term and thus be comparable to the characteristic time of the dynamic Stokes shift of about 2 ps at room temperature. However, as mentioned above, experimentally a residual lifetime of about 30 ps in ethanol (~130 ps in decanol) is found for auramine in the excited state.[224] We conclude that the time-resolved transients of auramine cannot be fully understood with the BFO model based on a nonemissive sink.

Alternatively, the possibility that the *radiative* (instead of the *nonradiative*) decay shows a functional dependence on the twisting angle of the phenyl rings was explored.[221] In this approach, the nature of the electronic wave function of the emissive excited state varies with the phenyl-group twisting angle. Such a situation may exist when adiabatic coupling between the (emissive) locally excited state and a dark state is assumed. Simulations of the temporal evolution of the excited-state population, again using a Smoluchowski equation but now without the sink function term, yielded spectra (dashed curves in Figure 20) in good agreement with the experimental spectra (solid curves in Figure 20). It appears that the best-fit results are obtained for a (quasi-) barrierless shape of the excited-state potential;[221] this potential indeed gives rise to a dynamic Stokes shift on a (sub)picosecond time scale. It also appeared that best-fit results were obtained when the rotational diffusion coefficient, D_r, in the Smoluchowsky equation is taken to be linearly dependent on T/η and therefore the Debye−Einstein−Stokes relation for rotational diffusion motion of a sphere, $D_r = k_B T/(12V\eta)$, is followed. The radius corresponding to this sphere is found as 1.0 Å, which compares well with the value of 1.2 Å for the effective radius of a twisting phenyl group.[221] The dark state has been identified as a twisted intramolecular charge transfer (TICT) state of auramine for which the emissive transition rate is negligible.[225]

Recently, the excited-state relaxation of auramine has also been studied for the solute in reverse micelle systems.[226,227] In the measurements, a pump−probe technique was applied in which the pump pulse generates a transient lens for the probe pulse. The pump-pulse induced change in the refractive index was measured as a change of the intensity of the

center area of the probe pulse and followed in time. Auramine was immersed in an aerosol OT/water/*n*-heptane reverse micelle system of nanometer-size. By means of the aforementioned ultrafast transient lens (UTL) method, two fast decay components for the relaxation of the excited state were found. The decay time constants were attributed to the decay of the locally excited (LE) and the twisted intramolecular charge transfer (TICT) state of auramine, respectively. The lifetimes of the two states vary with the size of the micelle water pool. As for the confined coumarine systems mentioned above, longer lifetimes were found as the radius of the water pool becomes smaller (up to 6 and 26 ps for the LE and TICT state in a water pool with a radius of ~0.7 nm, respectively).

3.2.2. Two-Dimensional Dynamics: Michler's Ketone

Recently, time-resolved fluorescence experiments have also been reported for the analogue compound of auramine, Michler's ketone (MK, Figure 21, 4,4′-bis(*N*,*N*-dimethylamino)-benzophenone) and its bridged derivative compound 3,6-bis(dimethylamino)-10,10-dimethylanthrone (BMK, Figure 21).[228,229] Fluorescence up-conversion transients were measured for MK and BMK in the protic solvents methanol, ethanol, and decanol, and in the aprotic solvents acetonitrile and DMF. The transients could be fitted with a multiexponential function convoluted with the system response function, and the best-fit functions were used to compute time-resolved fluorescence spectra by means of the spectral reconstruction procedure.[69,228] Figure 22 presents data for MK in various protic solvents. The solid curves are best-fit curves for the simulated points to log-normal line shape functions.[228] The time dependence of the fluorescence spectrum of MK in alcoholic solution shows (i) a dynamic Stokes shift to lower energies on a (sub)picosecond time scale (after about 5 ps, the emission band maximum for MK in methanol and ethanol is even red-shifted with respect to the band maximum of the steady-state fluorescence spectrum showing that the latter is dominated by fluorescence from nonrelaxed molecules (Figure 22a,b)), (ii) a slower dynamics in the order methanol, ethanol, and decanol, and (iii) a decrease of the total integrated emission intensity concomitant with the dynamic Stokes shifts. In the aprotic solvents acetonitrile and DMF, the MK fluorescence transients also yield a dynamic Stokes shift accompanied by a decrease in the total emission intensity. However, after about 50 ps the shifting of the band maximum is over and a residual emission is observed. This residual component decays with a time of 800 ps typical of the lifetime of the relaxed excited state of MK. Figure 22d shows the time dependence of the emission spectrum of BMK in ethanol, also obtained after spectral reconstruction. From the time dependences of the first moments of the reconstructed emission bands for MK and BMK, the parameters listed in Table 6 were obtained.

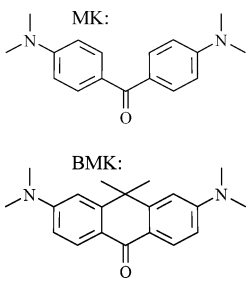

Figure 21. Structures of 4,4′-bis(*N*,*N*′-dimethylamino)-benzophenone (MK) and its bridged derivative 3,6-bis-(dimethylamino)-10,10-dimethylanthrone (BMK).

Several possibilities may be mentioned to explain the similar dynamics for the Stokes shift and the integrated fluorescence intensity decay of MK in protic solution. Both observables appear sensitive to the viscosity of the solvent (compare, for example, the dynamics of the Stokes shift for MK in methanol, ethanol, and decanol (Figure 22a−c, Table 6)). First, the dynamic Stokes shift could result from solvation. However, a decay of the fluorescence intensity concomitant with the DSS of MK is generally not expected since the nature of the emissive electronic state usually does not change with the reorientational motions of the solvent molecules. It could be, however, that the lifetime of the emissive state is coincidentally of the order of the characteristic time of the Stokes shift. This latter possibility could be excluded since the integrated emission intensity of the time-dependent reconstructed emission spectra against the frequency (in cm^{-1}) of the optical transition for MK dissolved in ethanol does not follow the ν^3-dependence that is expected according to Einstein's relation for spontaneous emission (see insert of Figure 22b, which shows the integrated intensity (dotted curve) and as a reference to the eye a ν^3-intensity dependence (dashed curve)). It is concluded that the MK fluorescence does not have a single and constant radiative decay time as MK develops to its relaxed excited state. A "normal" solvation process in which only a dynamic Stokes shift is observed and in which the total integrated fluorescence intensity remains unaffected (apart from the ν^3 dependence) apparently does not apply in the case of MK.

Another possible cause for the picosecond dynamic Stokes shift of MK in alcoholic solution is (intramolecular) reorientational motions of the phenyl groups within the MK molecule. When a picture similar to that mentioned above for the analogue dye molecule, auramine, is adopted, the similar dynamics of the dynamic Stokes shift and the decay of the integrated fluorescence intensity may originate in the effect that intramolecular phenyl-group twisting has on the adiabatic coupling of an emissive LE state and a weakly- or nonemissive TICT state. Thus, as relaxation along the (quasi-) barrierless potential energy surface takes place, the nature of the electronic wave function varies from radiative to nonradiative.

The alternative that the enhanced decay of the fluorescence of MK is due to *nonradiative* decay has also been considered.[228] Formally, the enhanced radiationless decay can be taken into account by including a twisting angle dependent sink function term.[224,230] In the sink function approach, the excited-

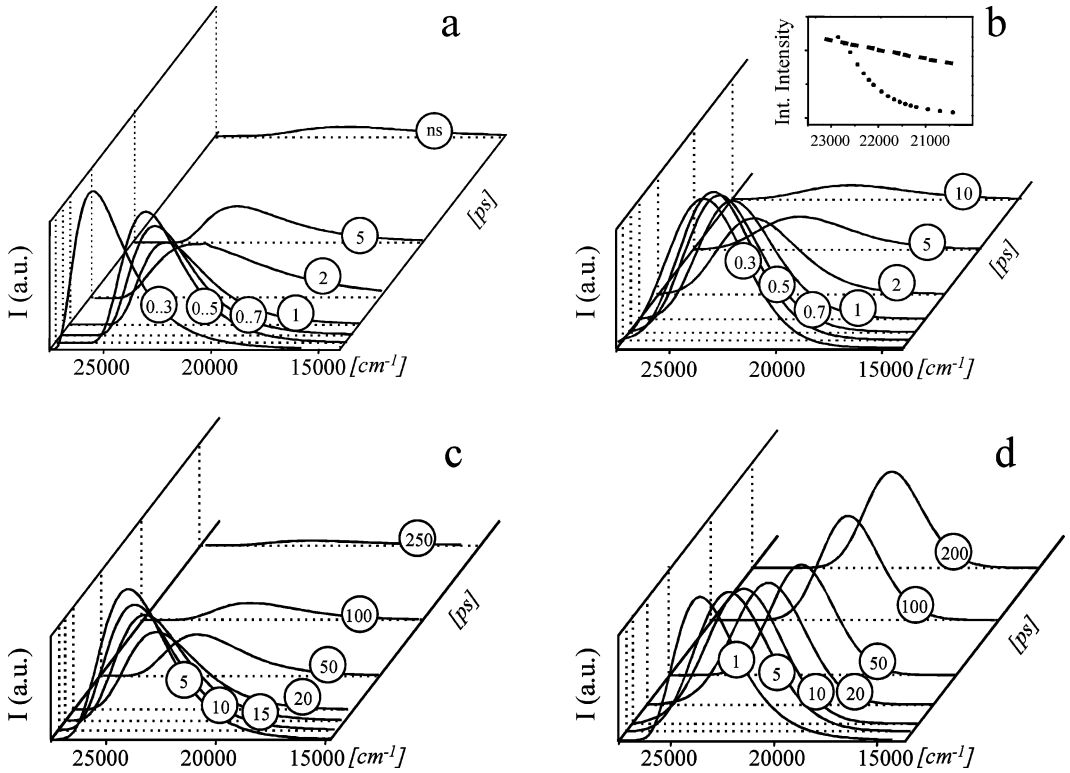

Figure 22. Time-resolved reconstructed fluorescence spectra of MK dissolved in (a) methanol, (b) ethanol and (c) decanol and (d) of BMK dissolved in ethanol. In the inset in panel b, the dots represent integrated intensity as a function of first moment of the reconstructed spectra of Michler's ketone in ethanol; the dashed line shows, as guide to the eye, a ν^3-dependence.

Table 6. Dynamic Stokes Shift (DSS, in cm^{-1}) and Weighted Characteristic Times (τ_{AV},[a] in ps) of DSS of Michler's Ketone (MK) and Blocked Michler's Ketone (BMK)[22]

	methanol				ethanol				decanol				DMF			
	DSS	τ_{AV}	τ_s[b]	τ_{int}[c]	DSS	τ_{AV}	τ_s[b]	τ_{int}[c]	DSS	τ_{AV}	τ_s[b]	τ_{int}[c]	DSS	τ_{AV}	τ_s[b]	τ_{int}[c]
MK	3500	3.1	5	2.0	2100	6	16	3.5	3200	104	245	48	5300	2.1	2	125
BMK					2100	16		680	2000	240		790	1000	2		490

[a] $\tau_{AV} = \sum a_i\tau_i/\sum a_i$, where a_i is the amplitude and τ_i is the time constant of the ith component in the biexponential fit of the DSS. [b] Solvation times (τ_s, in ps) are taken from ref 118. [c] Weighted decay times of the integrated fluorescence intensity.

state lifetime is twist angle dependent and in fact is shortest in the relaxed excited state. This, however, turned out not to be the case for MK, and thus, it was proposed that twisting of the phenyl groups is of dominant influence both on the dynamics of the Stokes shift and on the radiative decay.

For the bridged compound BMK, the time dependence of the fluorescence is quite different. Now the dynamics of the Stokes shift and the fluorescence intensity decay occur on different time scales (Table 6). Since bridging of the phenyl groups blocks the twisting motions in BMK, such motions cannot possibly cause the fast dynamic Stokes shift. On the other hand, the dynamic Stokes shift is solvent-dependent and thus may be due to solvation. In Table 6, the weighted average times for the multiexponential dynamic Stokes shift (τ_{AV}), as well as typical solvation times (τ_s) from the literature for the solvents used, are presented. The close similarity of τ_{AV} with τ_s is support that for BMK the dynamic Stokes shift is due to solvation.

A comparison of the kinetics of MK and BMK in the same alcohol (e.g., see the time constants in Table 6 for the dynamic Stokes shifts of MK and BMK in ethanol) shows that the dynamics for MK is more than 2 times faster. Hynes et al. have recently analyzed for TICT molecules that an enhancement in the dynamics of the Stokes shift may occur by considering in a two-dimensional approach the effects of twisting *and* solvation.[231−233] Several limiting cases were distinguished, including ones where solvent relaxation is either "slow"or "fast" with respect to the characteristic twisting time. In the slow-solvent limit, the reaction is started by solvation, but very soon twisting takes over and virtually determines the dynamics of the reaction. Nordio et al. have recently introduced a related approach differentiating between "fast" and "slow" solvents.[234] This approach is also applicable to barrierless reactions. As discussed above for MK, intramolecular twisting motions eventually determine the electronic character of the excited state and the dynamic Stokes shift. Within the two-dimensional approach, this implies that for MK the slow-solvent limit applies and as noted before, in this limit, fast twisting dominates eventually the dynamics of the Stokes shift. Such a mechanism is not conceivable for BMK, hence the faster dynamics for MK. The slow-solvent result for MK in

simple protic solvents like methanol and ethanol is somewhat surprising because in these solvents fast nuclear polarizations generally prevail due to the presence of high-frequency modes (30−50 ps^{-1}, ref 133). However, for MK it has been noted that in alcoholic solution an inhomogeneous distribution of stabilized twisted configurations may exist,[235] and it may be that the influence of the short-time dynamics of the solvent may be drastically changed and that long-time relaxation dynamics determines the role of the solvent as for TICT molecules.[133,236]

The kinetics of the fluorescence of MK in the aprotic solvents acetonitrile and DMF initially displays a very fast dynamic Stokes shift and concomitantly an intensity decay, but after about 50 ps, the steady-state emission is reached and the emission decays with the excited-state lifetime of 800 ps. In fact, the kinetics of the dynamic Stokes shift of MK and BMK in acetonitrile is so fast that only a very small fraction of this shift could be followed with time.[228] Due to this, reliable values of the parameters are missing in Table 6 for this solvent. Within the framework of the two-dimensional model,[231−234] it is thus found that for MK in aprotic solvents the fast solvation limit applies, that is, the solvation dynamics is much faster than the twisting reaction. In such a limit, initially the dynamics are governed by twisting motions but very quickly the reaction dynamics is dominated by the fast dynamics of the solvation process. Indeed, in acetonitrile and DMF, solvation times as short as 0.26 and 2.0 ps, respectively, have been reported.[118] Eventually, the excited state relaxes exponentially in accordance with the excited-state lifetime. For MK in DMF, the measured lifetime is found as 800 ps.

3.2.3. Coumaric Acid in Solution and Proteins

In nature, chromophores fulfill an important role in initiating signal transduction in a photoreceptor. After light absorption, the chromophore frequently undergoes ultrafast intramolecular conformational changes, for example, trans−cis isomerization, so the interaction of the chromophore with the protein environment is altered. At a later stage, this leads to the appearance of the signaling state and eventually the biological response. These phenomena have been extensively studied for rhodopsins,[237−239] bacteriorhodopsins,[240] and phytochromes[241,242] and have been reviewed in several papers.[211,243,244] Here we primarily focus on a few femtosecond fluorescence upconversion studies of coumaric acid (for structure, see insert of Figure 23a), which is the photoreceptor in wild-type photoactive yellow protein (PYP) and a few derivative protein systems.[245] In contrast to the results for the styryl dyes discussed in section 3.1, the coumaric acid chromophore in proteins is an example of a styryl dye chromophore for which fast transient fluorescence behavior is found to be due to intramolecular conformational changes and not to solvation. This is further detailed as follows.

PYP, isolated from the halophilic purple bacterium *Ectothiorhodospira halophila*,[246] has been identified as the pigment controlling negative phototaxis of bacteria. PYP contains a *p*-hydroxycinnamic acid

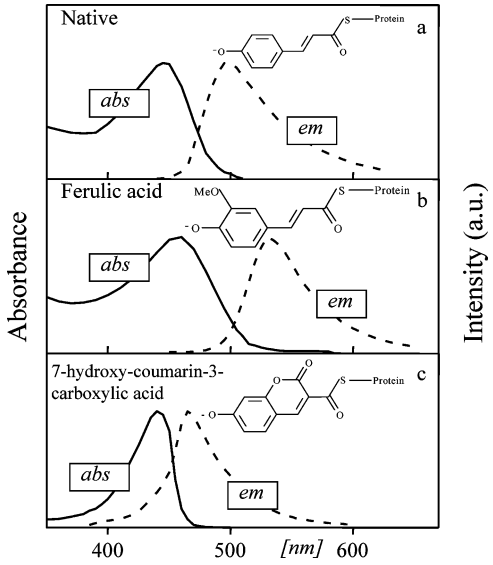

Figure 23. Steady-state absorption and fluorescence spectra of (a) native, (b) ferulic acid, and (c) 7-hydroxy-coumarin-3-carboxylic acid PYP dissolved in water (10 mM Tris·HCl, pH = 7.5). Inserts are the corresponding fluorophore structures.

chromophore[247,248] linked to a cysteine in the protein through a thiol ester bond[249] that is deprotonated in the ground state of PYP (Figure 23).[248,250] In the ground state, the PYP chromophore vinyl group is in the trans configuration.[247,250] Blue light absorption triggers a reversible photocycle in which several intermediate species are formed, one of which, the protonated chromophore pB, is believed to be representative of the signaling state.[244] In a study of the time dependence of the spontaneous fluorescence of PYP, a decay faster than about 12 ps was concluded.[251] Subsequent femtosecond fluorescence upconversion studies with orders of magnitude better time resolution showed a multiexponential fluorescence decay with typical times ranging from a few hundred femtoseconds to a few picoseconds.[245,252] The very fast fluorescence transients were interpreted to arise from fast barrierless trans−cis isomerization taking place inside the protein chromophore. This could be further tested from a comparison of the time-resolved fluorescence transients of native PYP and an artificial derivative, containing the 7-hydroxy-coumarin-3-carboxylic acid chromophore (Figure 23).[245] One would expect that if the structure of the chromophore is modified such that twisting motions around the relevant double bond in the probe molecule are blocked, this would result in a reduction of the relative magnitude of the (sub)picosecond component in the decay kinetics of the probed fluorescence.

Figure 24 shows representative fluorescence decays measured for native and the hybrid PYP. The fluorescence transient for native PYP shows an instantaneous rise and after deconvolution fitted a multiexponential decay function with time constants of about 700 fs (50%), 3 ps (30%), and 50 ps (20%). The PYP emission lacked a dynamic red shift. In contrast with the native protein results, the fluorescence of the 7-hydroxy-coumarin-3-carboxylic acid hybrid did not contain components shorter than 60 ps. The

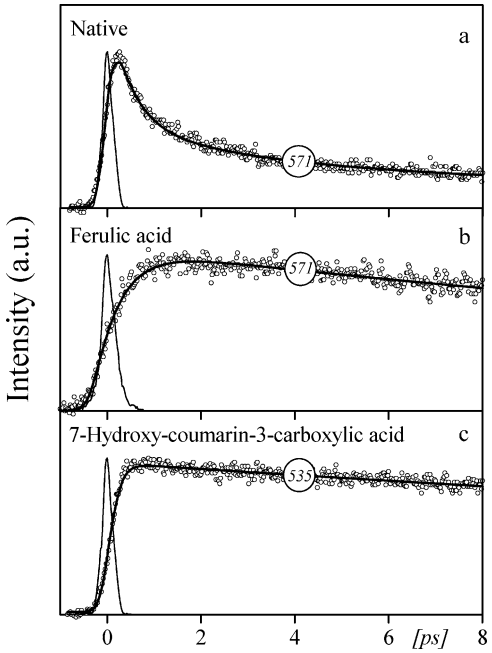

Figure 24. Representative fluorescence up-conversion transients of (a) native, (b) ferulic acid, and (c) 7-hydroxy-coumarin-3-carboxylic acid PYP dissolved in water (10 mM Tris·HCl, pH = 7.5). Solid curves are the best fits using a triexponential function. Instrumental response is shown also. Detection wavelengths (in nm) are given in circles.

fluorescence transient could be fitted to a convoluted multiexponential function with typical times of 58 ps (75%), 450 ps (9%), and 3.4 ns (16%).

The ultrafast appearance, the fast nonexponential decay, and the negligible red shift of the spontaneous emission of wild-type PYP show a behavior very similar to bacteriorhodopsin (bR).[230,253,254] To interpret the results for the chromophore in native PYP, a model analogous to that considered for retinal in bR[254] was proposed.[245] In this model, after pulsed photoexcitation, the decay out of the Franck−Condon regime is assumed to be very fast (<50 fs) and into an almost flat (nonrepulsive) excited-state potential, S_1. The S_1 state is now in a reactive region typical of a twisted chromophore molecule, where its potential energy surface shows an avoided crossing with that of S_2, after which the molecule may twist further and decay nonradiatively back into the trans or twist further into the cis conformation. Due to ill-defined surroundings of the chromophore in the protein pocket, in the avoided crossing region an inhomogeneity may be expected. This inhomogeneity will cause a spread in the twisting angle in the reactive region and since the twisting angle may strongly influence the excited-state lifetime, an inhomogeneous spread in the lifetime of the emissive state, S_1,will result. It is thus proposed that the multiexponential fluorescence decay of the chromophore in native PYP is due to an inhomogeneous distribution of lifetimes with values that may vary from 500 fs up to the picosecond time regime. For the 7-hydroxy-coumarin-3-carboxylic acid hybrid, the fast (700 fs and 3 ps) decay components, which are characteristic of the native PYP fluorescence decay, are missing. Obviously, the rigid ring structure of the chromophore now prevents trans−cis isomerization of the chromophore, and rapid decay into the reactive state cannot possibly take place.

Another modification of the chromophore molecule inside the protein, where now a methoxy group was attached to the phenyl group of the coumaric acid (at the meta position with respect to the vinyl group), has also been examined.[245] For this ferulic acid PYP hybrid sample, the fluorescence again showed a fast multiexponential decay with components of about 0.7−3 ps at the blue side of the emission band. At the red wing, no ultrafast decay components were detected. Moreover, an enhanced spectral broadening was observed. The data are consistent with a picture in which the ferulic acid chromophore fits less well in the protein pocket, causing an inhomogeneous spread in the decay times and also an inhomogeneous spectral broadening of the emission. When the substituent was a hydroxyl instead of the methoxy group, that is, the chromophore was caffeic acid, the results were similar to those for the ferulic acid hybrid.[255] This again illustrates that a subtle change in the chromophore structure may be of appreciable influence to the temporal and spectral behavior of the hybrid.

The influence of chemical changes of the vinyl group on the isomerization dynamics has also been investigated.[255] In particular, for PYP containing a deuterated or brominated vinyl group at the *p*-coumaric acid site, the time dependence of the fluorescence was examined. Neither deuteration nor bromination had any effect on the fluorescence kinetics compared with native PYP. The results indicated that the inertial moment of the vinyl group is not relevant for the isomerization process. This could imply that twisting, later followed by isomerization, of the chromophore in the protein is not restricted to the double bond but may be controlled by additional atomic rearrangements. This was also suggested on the basis of FTIR experiments,[256,257] cryotrapping X-ray experiments,[258] and site-directed mutagenesis experiments.[259,260] In the latter (fluorescence up-conversion) experiments, Chosrowjan et al. compared the fluorescence dynamics of (deprotonated) *p*-coumaric acid in aqueous solution with that of the chromophore in wild-type PYP. The results strongly suggest that the rate of formation of the twisted state is much more enhanced in the nanospace of the protein pocket than in aqueous solution where solvation also plays a role. Also, in PYP mutants with a probably looser structure, because of weakening of the chromophore−amino acid residue hydrogen bonding, the ultrafast processes (flipping of thioester linkage and vinyl group isomerization) leading to the twisted configuration are slowed. It seems that native PYP is engineered to optimize the twisting of the chromophore. Lack of temperature activation suggested a barrierless or coherent twisting process. Very recently, coherent oscillatory behavior was reported in the fluorescence transients detected at the blue and red edges of the wild-type PYP emission band.[261] Transient absorption experiments of several model systems that mimic the PYP chromophore have also been performed recently.[262,263] For deprotonated *trans*-coumaric acid in basic aqueous solution

(pCA^{2-}), a photoinduced trans−cis isomerization with a time constant of about 10 ps was reported. As in the up-conversion experiments for the denatured PYP,[259] but in contrast with the results for native PYP,[245,252] no intermediate twisted configuration could be found; the trans−cis isomerization process was much slower than that for the native PYP chromophore. However, the transient absorption and gain results for *trans*-*S*-phenyl thio-*p*-hydroxycinnamate anion (pCT^{-}) could more adequately simulate those for the native PYP chromophore, probably because the chromophore also contains the thioester functional group.[263] Now the excited-state relaxation proceeds through the rapid formation, within 1.7 ps, of an intermediate (not found for pCA^{2-}) that decays in 2.8 ps to form a long-lived photoproduct tentatively assigned as the *cis*-chromophore isomer. A general conclusion is that to understand the intricate details of the photodynamics in wild-type PYP one has to consider the intrinsic properties of both the chromophore and the protein environment.

Ultrafast photoisomerization reactions have been studied for many other photoactive proteins. Perhaps the most extensively examined chromophore is retinal in rhodopsin (where it is involved in the initiation of the vision process in the human eye) and bacteriorhodopsin (where it serves to drive photosynthesis). A review of recent ultrafast work of chromophores in proteins[242,243,264−267] and pigments in plants[268−271] is outside the scope of this paper, however.

4. Concluding Remarks

Investigations of ultrafast processes are of great importance for unravelling details of the mechanisms of molecular relaxation of large-sized molecules. In the condensed phase, both intra- and intermolecular interactions are important in the relaxation mechanisms. High-tech developments in laser technology have been crucial for the feasibility of ultrafast studies. Nowadays processes as fast as ∼20 fs can be investigated. For the large-sized chromophores discussed in section 3, the excited-state dynamics could be classified as due to either solvation, intramolecular configurational changes, or both. For the probe molecules showing predominantly solvation dynamics, ultrafast inertial free streaming (∼50−100 fs) and rotational diffusion (a few picoseconds) contributions to the transient absorption or fluorescence up-conversion spectra could be discerned when the experimental time resolution was better than 100 fs. From the results for molecules such as DCM, DASPI, and C153, it is also clear that at the shortest time scales (∼10−60 fs), the separation of contributions of intramolecular vibrational relaxation on one hand and solvation on the other hand is still an issue under debate. Also, as illustrated by the examples of auramine, Michler's ketone, and bridged Michler's ketone, a clear-cut distinction into excited-state dynamics due to intramolecular and environmental mode contributions cannot always be made. In practice, due to the entanglement of both kinds of contributions, a multidimensional approach is necessary to explain the results. Likewise, a simple one-dimensional photoisomerization of the all-trans to 13-cis configuration of retinal in bacteriorhodopsin is unlikely since the analogue of native bR, named blocked-bR, in which the C_{13}═C_{14} chromophore isomerization is blocked, shows similar excited-state dynamics during the first few hundred femtoseconds.[272−274] A multidimensional potential energy surface was also invoked for explaining the results of polarized pump−probe experiments for bovine rhodopsin.[275] Ultrafast fluorescence up-conversion experiments recently performed for mono- and dichromo hemicyanine dyes also indicated that the dynamic Stokes shift involves not only solvation dynamics but also TICT formation.[276] Much further work, both experimentally and theoretically, is needed to better understand the implications and ubiquity of multidimensional mode dynamics.

As for the near future, it is expected that ultrafast studies of chromophores will be directed more and more to systems of increasing complexity. Examples of such complex systems are dendrimers,[277] porphyrin aggregates,[48,49,278−280] flavines,[281] proteins (e.g., green fluorescent protein[267,282−285]), and many other complex systems. In many of these studies, special attention is given to the different types of solvation trajectories: solvation due to bulk solvent molecules and due to solvent molecules at the surface of the biomolecule (e.g., protein), micelle, vesicle, aggregate, etc.[147,148] Chromophores have also been extensively applied in studies of *inter*molecular electron-transfer dynamics in electron donor−acceptor complexes.[286−291] Also, ultrafast processes in newly designed materials such as nanocrystals (AgBr, TiO_2, CdSe) sensitized with dye molecules are under investigation.[292−294] Finally, ultrafast fluorescence methods have recently been applied in investigations of the dynamics of chiral self-assembling of polymer aggregates[295] and new tags in biopolymers.[296] No doubt, considering the rapid progress that has been made in recent years, both in ultrafast laser technology and in materials science, many exciting new applications of large chromophore systems will continue to emerge within chemistry and biology for many years to come.

5. References

(1) Drexhage, K. H. *Top. Appl. Phys.* **1973**, *1*, 144.
(2) Schäfer, F. P. *Top. Appl. Phys.* **1992**, *70*, 19.
(3) Reichardt, C. *Chem. Rev.* **1994**, *94*, 2319.
(4) Rettig, W. *Angew. Chem., Int. Ed. Engl.* **1986**, *25*, 971.
(5) Rettig, W.; Rurack, K.; Sczepan, M., In *New Trends in Fluorescence Spectroscopy*; Valeur, B., Brochon, J.-C., Eds.; Springer: Heidelberg, Germany, 2001; pp 125−156.
(6) Bell, T. W.; Hou, Z.; Drew, M. G.; Chaopoteau, E.; Czech, B. P.; Kumar, A. *Science* **1995**, *269*, 671.
(7) Adam, S. R.; Harootunian, A. T.; Buechler, Y. J.; Taylor, S. S.; Tsien, R. Y. *Nature* **1991**, *349*, 694.
(8) Klonkowski, A. M.; Kledzik, K.; Ostaszewski, R.; Jezierska, J. *Appl. Surf. Sci.* **2002**, *196*, 383.
(9) Kim, S. K.; Bang, M. Y.; Lee, S. H.; Nakamura, K.; Cho, S. W.; Yoon, J. *J. Inclusion Phenom. Macrocyclic Chem.* **2002**, *43*, 71.
(10) Chiba, M.; Kim, H. B.; Kitamura, N. *J. Photochem. Photobiol., A* **2002**, *151*, 67.
(11) Liao, J. H.; Chen, C. T.; Fang, J. M. *Org. Lett.* **2002**, *4*, 561.
(12) Rudzinski, C. M.; Young, A. M.; Nocera, D. G. *J. Am. Chem. Soc.* **2002**, *124*, 1723.
(13) Tong, H.; Wang, L. X.; Jing, X. B.; Wang, F. *Macromol. Rapid Commun.* **2002**, *23*, 877.
(14) Armaroli, N.; Accorsi, G.; Gisselbrecht, J. P.; Gross, M.; Krasnikov, V.; Tsamouras, D.; Hadziioannou, G.; Gomez-Escalonilla, M. J.; Langa, F.; Eckert, J. F.; Nierengarten, J. F. *J. Mater. Chem.* **2002**, *12*, 2077.

(15) Kalny, D.; Elhabiri, M.; Moav, T.; Vaskevich, A.; Rubinstein, I.; Shanzer, A.; Albrecht-Gary, A. M. *Chem. Commun.* **2002**, *13*, 1426.
(16) Bissell, R. A.; Cordova, E.; Kaifer, A. E.; Stoddart J. F. *Nature* **1994**, *369*, 133.
(17) Raymo, F. M.; Giordani, S. *Org. Lett.* **2001**, *3*, 1833.
(18) Lammi, R. K.; Wagner R. W.; Ambroise, A.; Diers, J. R.; Bocian, D. F.; Holten, D.; Lindsey, J. S. *J. Phys. Chem. B* **2001**, *105*, 5341.
(19) Osuka, A.; Fujikane, D.; Shinmori, H.; Kobatake, S.; Irie, M. *J. Org. Chem.* **2001**, *66*, 3913.
(20) Bulović, V.; Shoustikov, A.; Baldo, M. A.; Bose, E.; Kozlov, V. G.; Thompson, M. E.; Forrest, S. R. *Chem. Phys. Lett.* **1998**, *287*, 455.
(21) Bulović, V.; Deshpande, R.; Thompson, M. E.; Forrest, S. R. *Chem. Phys. Lett.* **1999**, *308*, 317.
(22) Mishra, A.; Behera, R. K.; Behera, P. K.; Mishra, B. K.; Behera, G. B. *Chem. Rev.* **2000**, *100*, 1973.
(23) Halls, J. J. M.; Pichler, K.; Friend, R. H.; Moratti, S. C.; Holmes, A. B. *Appl. Phys. Lett.* **1996**, *68*, 3120.
(24) Yu, G.; Heeger, A. J. *J. Appl. Phys.* **1995**, *78*, 4510.
(25) Shi, J.; Tang, C. W. *Appl. Phys. Lett.* **1997**, *70*, 1665.
(26) Chung, J.; Chio, B.; Lee, H. H. *Appl. Phys. Lett.* **1999**, *74*, 3645.
(27) Kido, J.; Matsumoto, T. *Appl. Phys. Lett.* **1998**, *73*, 2866.
(28) Barbara, P. F.; Jarzeba, W. *Adv. Photochem.* **1990**, *15*, 1.
(29) Bagchi, B. *Annu. Rev. Phys. Chem.* **1989**, *40*, 115.
(30) Yoshihara, K. *Adv. Chem. Phys.* **1999**, *107*, 371.
(31) Yoshihara, K.; Tominaga, K.; Nagasawa, Y. *Bull. Chem. Soc. Jpn.* **1995**, *68*, 696.
(32) Marcus, R. A. *Annu. Rev. Phys. Chem.* **1964**, *15*, 155.
(33) Marcus, R. A.; Sutin, N. *Biochim. Biophys. Acta* **1985**, *811*, 265.
(34) Bixon, M.; Jortner, J. *Chem. Phys.* **1993**, *176*, 467.
(35) Tolbert, L. M.; Solntsev, K. M. *Acc. Chem. Res.* **2002**, *35*, 19.
(36) Chien, Y. Y.; Wong, K. T.; Chou, P. T.; Cheng, Y. M. *Chem. Commun.* **2002**, *23*, 2874.
(37) Elsaesser, T. Ultrafast excited-state hydrogen transfer in the condensed phase. In *Ultrafast hydrogen bonding dynamics and proton transfer processes in the condensed phase*; Elsaesser, T., Bakker, H. J., Eds.; Kluwer Academic Publishers: Dordrecht, The Netherlands, 2002; pp 119−153.
(38) Toele, P.; Zhang, H.; Glasbeek, M. *J. Phys. Chem. A* **2002**, *106*, 3651.
(39) Fiebig, T.; Chachisvilis, M.; Manger, M.; Zewail, A. H.; Douhal, A.; Garcia-Ochoa, I.; Ayuso, A. D. H. *J. Phys. Chem. A* **1999**, *103*, 7419.
(40) Ameer-Beg, S.; Ormson, S. M.; Brown, R. G.; Matousek, P.; Towrie, M.; Nibbering, E. T. J.; Foggi, P.; Neuwahl, F. V. R. *J. Phys. Chem. A* **2001**, *105*, 3709.
(41) Rettig, W.; Maus, M. Conformational changes accompanying intramolecular excited-state electron transfer. In *Conformational Analysis of Molecules in Excited States*; Waluk, J., Ed.; Wiley-VCH: New York, 2000.
(42) Rini, M.; Kummrow, A.; Dreyer, J.; Nibbering, E. T. J.; Elsaesser, T. *Faraday Discuss.* **2003**, *122*, 27.
(43) Liu, R. S. H. *Photochem. Photobiol.* **2002**, *76*, 580.
(44) Stratt, R. M.; Maroncelli, M. *J. Phys. Chem.* **1996**, *100*, 12981.
(45) Deng, Y.; Stratt, R. M. *J. Chem. Phys.* **2002**, *117*, 1735.
(46) Owrutsky, J. C.; Raftery, D.; Hochstrasser, R. M. *Annu. Rev. Phys. Chem.* **1994**, *45*, 519.
(47) Oxtoby, D. W. *Adv. Chem. Phys.* **1981**, *47*, 487.
(48) Baskin, J. S.; Yu, H. Z.; Zewail A. H. *J. Phys. Chem. A* **2002**, 106, 9837.
(49) Yu, H. Z.; Baskin, J. S.; Zewail, A. H. *J. Phys. Chem. A* **2002**, *106*, 9845.
(50) Foggi, P.; Neuwahl, F. V. R.; Moroni, L.; Salvi, P. R. *J. Phys. Chem. A* **2003**, *107*, 1689.
(51) Rini, M.; Holm, A. K.; Nibbering, E. T. J.; Fidder, H. *J. Am. Chem. Soc.* **2003**, *125*, 3028.
(52) Siebert, T.; Maksimenka, R.; Materny, A.; Engel, V.; Kiefer, W.; Schmitt, M. *J. Raman Spectrosc.* **2002**, *33*, 844.
(53) Bagchi, B.; Biswas, R. *Adv. Chem. Phys.* **1999**, *109*, 207.
(54) de Boeij, W. P.; Pshenichnikov, M. S.; Wiersma, D. A. *Annu. Rev. Phys. Chem.* **1998**, *49*, 99.
(55) Fleming, G. R.; Cho, M. H. *Annu. Rev. Phys. Chem.* **1996**, *47*, 109.
(56) Fainberg, B. D.; Huppert, D. *Adv. Chem. Phys.* **1999**, *107*, 191.
(57) Rulliere, C., Ed., *Femtosecond Laser Pulses. Principles and Experiments*; Springer: Berlin, 1998.
(58) Herrmann, J.; Wilhelmi, B. *Lasers for Ultrashort Light Pulses*; North-Holland: Amsterdam, 1987.
(59) Demtröder, W. *Laser Spectroscopy*, 3rd ed; Springer: Berlin, 2003.
(60) Mukamel, S. *Principles of Nonlinear Spectroscopy*; Oxford University Press: New York, 1995.
(61) See, for example, contributions in: Manz, J., Wöste, L., Eds. *Femtosecond Chemistry I and II*; VCH: Weinheim, Germany, 1995.
(62) May, V.; Kühn, O. *Charge and Energy Transfer Dynamics in Molecular Systems*; Wiley-VCH: Weinheim, Germany, 1999.
(63) Bixon, M.; Jortner, J. *Adv. Chem. Phys.* **1999**, *106*, 35.
(64) Zewail, A. H. *J. Phys. Chem. A* **2000**, *104*, 5660.
(65) Castner, E. W., Jr.; Maroncelli, M.; Fleming, G. R. *J. Chem. Phys.* **1987**, *86*, 1090.
(66) Maroncelli, M. *J. Mol. Liq.* **1993**, *57*, 1.
(67) Castner, E. W., Jr.; Maroncelli, M. *J. Mol. Liq.* **1998**, *77*, 1.
(68) Hartman, R. S.; Konitsky, W. M.; Waldeck, D. H.; Chang, Y. J.; Castner, E. W., Jr. *J. Chem. Phys.* **1997**, *106*, 7920.
(69) Maroncelli, M.; Fleming, G. R. *J. Chem. Phys.* **1987**, *86*, 6221.
(70) Rosenthal, S. J.; Jimenez, R.; Fleming, G. R., Kumar, P. V.; Maroncelli, M. *J. Mol. Liq.* **1994**, *60*, 25.
(71) Kahlow, M. A.; Kang, T. J.; Barbara, P. F. *J. Chem. Phys.* **1988**, *88*, 2372.
(72) Jarzeba, W.; Walker, G. C.; Johnson, A. E.; Barbara, P. F. *Chem. Phys.* **1991**, *152*, 57.
(73) Rotkiewicz, K.; Grellmann, K. H.; Grabowski, Z. R. *Chem. Phys. Lett.* **1973**, *19*, 315.
(74) Grabowski, Z. R. *Pure Appl. Chem.* **1992**, *64*, 1249.
(75) Grabowski, Z. R. *Pure Appl. Chem.* **1993**, *65*, 1751.
(76) Laenen, R.; Rauscher, C.; Laubereau, A. *Chem. Phys. Lett.* **1998**, *283*, 7.
(77) Gaffney, K. J.; Piletic, I. R.; Fayer, M. D. *J. Phys. Chem. A* **2002**, *106*, 9428.
(78) Levinger, N. E.; Davis, P. H.; Behera, P. K.; Myers, D. J.; Stromberg, C.; Fayer, M. D. *J. Chem. Phys.* **2003**, *118*, 1312.
(79) Rubtsov, I. V.; Hochstrasser, R. M. *J. Phys. Chem.* B **2002**, *106*, 9165.
(80) Heyne, K.; Huse, N.; Nibbering, E. T. J.; Elsaesser, T. *Chem. Phys. Lett.* **2003**, *369*, 591.
(81) Deak, J. C.; Iwaki, L. K.; Rhea, S. T.; Dlott, D. D. *J. Raman Spectrosc.* **2000**, *31*, 263.
(82) Bardeen, C. J.; Wang, Q.; Shank, C. V. *J. Phys. Chem. A* **1998**, *102*, 2759.
(83) Tomov, I. V.; Oulianov, D. A.; Chen, P. L.; Rentzepis, P. M. *J. Phys. Chem. B* **1999**, *103*, 7081.
(84) Brown, F. L. H.; Wilson, K. R.; Cao, J. S. *J. Chem. Phys.* **1999**, *111*, 6238.
(85) Chen, L. X.; Jager, W. J. H.; Jennings, G.; Gosztola, D. J.; Munkholm, A.; Hessler, J. P. *Science* **2001**, *292*, 262.
(86) Bressler, C.; Saes, M.; Chergui, M.; Grolimund, D.; Abela, R.; Pattison, P. *J. Chem. Phys.* **2002**, *116*, 2955.
(87) Pollard, W. T.; Mathies, R. A. *Annu. Rev. Phys. Chem.* **1992**, *43*, 497.
(88) Shah, J. *IEEE J. Quantum Electron.* **1988**, *24*, 276.
(89) Kahlow, M. A.; Jarzeba, J.; DuBruil, T. P.; Barbara, P. F. *Rev. Sci. Instrum.* **1988**, *59*, 1098.
(90) Mialocq, J.-C.; Gustavsson, T. In *New Trends in Fluorescence Spectroscopy*; Valeur, B., Brochon, J.-C., Eds., Springer: Heidelberg, Germany, 2001; pp 61−80.
(91) Schanz, R.; Kovalenko, S. A.; Kharlanov, V.; Ernsting, N. P. *Appl. Phys. Lett.* **2001**, *79*, 566.
(92) Lakowicz, J. R. *Principles of Fluorescence Spectroscopy*; Plenum: New York, 1999.
(93) Szabo, A. *J. Chem. Phys.* **1984**, *81*, 150.
(94) Wynne, K.; Hochstrasser, R. M. *Chem. Phys.* **1993**, *171*, 179.
(95) Bakshiev, N. G. *Opt. Spectrosc.* **1964**, *16*, 446.
(96) Bakshiev, N. G.; Mazurenko, Y. T.; Pieterskaya, I. *Opt. Spectrosc.* **1966**, *21*, 307.
(97) Mazurenko, Y. T.; Bakshiev, N. G. *Opt. Spectrosc.* **1970**, *28*, 905.
(98) Ware, W. R.; Lee, S. K.; Brant, G. J.; Chow, P. P. *J. Chem. Phys.* **1971**, *54*, 4729.
(99) Chakrabarti, S. K.; Ware, W. R. *J. Chem. Phys.* **1971**, *55*, 5494.
(100) Ware, W. R.; Chow, P. P.; Lee, S. K. *Chem. Phys. Lett.* **1968**, *2*, 356.
(101) Hynes, J. T. *J. Phys. Chem.* **1986**, *90*, 3701.
(102) Kubo, R.; Toda, M.; Hashitsume, N. *Statistical Physics II*; Springer: New York, 1991.
(103) Chandler, D. *Introduction to Modern Statistical Mechanics*; Oxford University Press: Oxford, U.K., 1987.
(104) Ladanyi, B. M.; Klein, S. *J. Chem. Phys.* **1996**, *105*, 1552.
(105) Ladanyi, B. M.; Stratt, R. M. *J. Phys. Chem.* **1996**, *100*, 1266.
(106) Cho, M.; Fleming, G. R.; Saito, S.; Ohmine, I.; Stratt, R. M. *J. Chem. Phys.* **1994**, *100*, 6672.
(107) Berlman, I. B. *Handbook of fluorescence spectra of aromatic molecules*; Academic Press: New York, 1971; pp 21−28.
(108) Mialocq, J.-C.; Meyer, M. *Laser Chem.* **1990**, *10*, 277.
(109) Pommeret, S.; Gustavsson, T.; Naskrecki, R.; Baldacchino, G.; Mialocq, J.-C. *J. Mol. Liq.* **1995**, *64*, 101.
(110) Meyer, M.; Mialocq, J.-C.; Perly, B. *J. Phys. Chem.* **1990**, *94*, 98.
(111) Hammond, P. R. *Opt. Commun.* **1979**, *29*, 331.
(112) Marason, E. G. *Opt. Commun.* **1981**, *37*, 56.
(113) Meyer, M.; Mialocq, J.-C. *Opt. Commun.* **1987**, *64*, 264.
(114) Drake, J. M.; Lesiecki, M. L.; Camaioni, D. M. *Chem. Phys. Lett.* **1985**, *113*, 530.
(115) Mialocq, J.-C.; Armand, X.; Marguet, S. *J. Photochem. Photobiol., A* **1993**, *69*, 351.
(116) Easter, D. C.; Baronavski, A. P. *Chem. Phys. Lett.* **1993**, *201*, 153.

(117) Mialocq, J.-C.; Pommeret, S.; Naskrecki, R.; Baldacchino, G.; Gustavsson, T. *SPIE* **1994**, *2370*, 253.
(118) Horng, M. L.; Gardecki, J.; Papazyan, A.; Maroncelli, M. *J. Phys. Chem.* **1995**, *99*, 17311.
(119) Kovalenko, S. A.; Ernsting, N. P.; Ruthman, J. *Chem. Phys. Lett.* **1996**, *258*, 445.
(120) Martin, M. M.; Plaza, P.; Meyer, Y. H.; Badaoui, F.; Bourson, J.; Lefevre, J. P.; Valeur, B. *J. Phys. Chem.* **1996**, *100*, 6879.
(121) Martin, M. M.; Plaza, P.; Changenet, P.; Meyer, Y. H. *J. Photochem. Photobiol. A* **1997**, *105*, 197.
(122) Martin, M. M.; Plaza, P.; Meyer, Y. H. *Chem. Phys.* **1995**, *192*, 367.
(123) Maciejewski, A.; Naskrecki, R.; Lorenc, M.; Ziolek, M.; Karolczak, J.; Kubicki, J.; Matysiak, M.; Szymanski, M. *J. Mol. Struct.* **2000**, *555*, 1.
(124) Mialocq, J.-C.; Armand, X.; Marguet, S. *J. Photochem. Photobiol., A* **1993**, *69*, 351.
(125) Zhang, H.; Jonkman, A. M.; van der Meulen, P.; Glasbeek, M. *Chem. Phys. Lett.* **1994**, *224*, 551.
(126) van der Meulen, P.; Zhang, H.; Jonkman, A. M.; Glasbeek, M. *J. Phys. Chem.* **1996**, *100*, 5367.
(127) Gustavsson, T.; Baldacchino, G.; Mialocq, J.-C.; Pommeret, S. *Chem. Phys. Lett.* **1995**, *236*, 587.
(128) Rosenthal, S. J.; Jimenez, R.; Fleming, G. R.; Kumar, P. V.; Maroncelli, M. *J. Mol. Liq.* **1994**, *60*, 25.
(129) Bingemann, D.; Ernsting, N. P. *J. Chem. Phys.* **1995**, *102*, 2691.
(130) Jimenez, R.; Fleming, G. R.; Kumar, P. V.; Maroncelli, M. *Nature* **1994**, *369*, 471.
(131) Carter, E. A.; Hynes, J. T. *J. Chem. Phys.* **1991**, *94*, 5961.
(132) Neria, E.; Nitzan, A. *J. Chem. Phys.* **1992**, *96*, 5433.
(133) Fonseca, T.; Ladanyi, B. M. *J. Phys. Chem.* **1991**, *95*, 2116.
(134) Cho, M.; Rosenthal, S. J.; Scherer, N. F.; Ziegler, L. D.; Fleming, G. R. *J. Chem. Phys.* **1992**, *96*, 5033.
(135) Yoshizawa, M.; Kubo, M.; Kurosawa, M. *J. Lumin.* **2000**, *87*−*89*, 739.
(136) van der Meulen, P.; Jonkman, A. M.; Glasbeek, M. *J. Phys. Chem. A* **1998**, *102*, 1906.
(137) Boldrini, B.; Cavalli, E.; Painelli, A.; Terenziani, F. *J. Phys. Chem. A* **2002**, *106*, 6286.
(138) Matyushov, D. V. *J. Chem. Phys.* **2001**, *115*, 8933.
(139) Milischuk, A.; Matyushov, D. V. *J. Phys. Chem. A* **2002**, *106*, 2146.
(140) Matyushov, D. V.; Newton, M. D. *J. Phys. Chem. A* **2001**, *105*, 8516.
(141) Pal, S. K.; Mandal, D.; Sukul, D.; Bhattacharyya, K. *Chem. Phys. Lett.* **1999**, *312*, 178.
(142) d'Angelo, M.; Fioretto, D.; Onori, G.; Palmieri, L.; Santucci, A. *Phys. Rev. E* **1996**, *54*, 993.
(143) Mandal, D.; Sen, S.; Bhattacharyya, K.; Tahara, T. *Chem. Phys. Lett.* **2002**, *359*, 77.
(144) Pal, S. K.; Sukul, D.; Mandal, D.; Sen, S.; Bhattacharyya, K. *Chem. Phys. Lett.* **2000**, *327*, 91.
(145) Pal, S. K.; Mandal, D.; Sukul, D.; Sen, S.; Bhattacharyya, K. *J. Phys. Chem. B* **2001**, *105*, 1438.
(146) Sen, S.; Dutta, P.; Mukherjee, S.; Bhattacharyya, K. *J. Phys. Chem. B* **2002**, *106*, 7745.
(147) Nandi, N.; Bhattacharyya, K.; Bagchi, B. *Chem. Rev.* **2000**, *100*, 2013.
(148) Pal, S. K.; Peon, J.; Bagchi, B.; Zewail, A. H. *J. Phys. Chem. B* **2002**, *106*, 12376.
(149) Changenet-Barret, P.; Choma, C. T.; Gooding, E. F.; DeGrado, W. F.; Hochstrasser, R. M. *J. Phys. Chem. A* **2000**, *104*, 9322.
(150) Brauns, E. B.; Madaras, M. L.; Coleman, R. S.; Murphy, C. J.; Berg, M. A. *J. Am. Chem. Soc.* **1999**, *121*, 11644.
(151) Jonkman, A. M.; van der Meulen, P.; Zhang, H.; Glasbeek, M. *Chem. Phys. Lett.* **1996**, *256*, 21.
(152) Yan, Y. J.; Mukamel, S. *J. Chem. Phys.* **1988**, *89*, 5160.
(153) Rosenthal, S. J.; Xie, X.; Du, M.; Fleming, G. R. *J. Chem. Phys.* **1991**, *95*, 4715.
(154) van der Meer, M. J.; Zhang, H.; Rettig, W.; Glasbeek, M. *Chem. Phys. Lett.* **2000**, *320*, 673.
(155) Fabian, J.; Nakazumi, H.; Matsuoka, M. *Chem. Rev.* **1992**, *92*, 1197.
(156) Brackmann, U. *Lambdachrome Laser Dyes*, 2nd ed.; Lambda Physik: Göttingen, Germany, 1994.
(157) Fromherz, P.; Dambacher, K. H.; Ephardt, H.; Lambacher, A.; Müller, C. O.; Neigle, R.; Schaden, H.; Schenk, O.; Vetter, T. *Ber. Bunsen-Ges. Phys. Chem.* **1991**, *95*, 1333.
(158) Narang, U.; Zhao, C. F.; Bhawalkar, J. D.; Bright, F. V.; Prasad, P. N. *J. Phys. Chem.* **1996**, *100*, 4521.
(159) Wang, H.; Zhang, H.; Rettig, W.; Tolmachev, A. I.; Glasbeek, M. *Phys Chem. Chem. Phys.*, submitted.
(160) Takeuchi, S.; Tahara, T. *Chem. Phys. Lett.* **1997**, *277*, 340.
(161) Gurzadyan, G. G.; Tran-Thi, T.-H.; Gustavsson, T. *J. Chem. Phys.* **1998**, *108*, 385.
(162) Kovalenko, S. A.; Ernsting, N. P.; Ruthmann, J. *J. Chem. Phys.* **1997**, *106*, 3504.
(163) Smith, N. A.; Meech, S. R.; Rubtsov, I. V.; Yoshihara, K. *Chem. Phys. Lett.* **1999**, *303*, 209.
(164) Weiss, M. N.; Srivastava, R.; Correia, R. R. B.; Martins-Filho, J. F.; de Arujo, C. B. *Appl. Phys. Lett.* **1996**, *69*, 3653.
(165) Casalboni, M.; De Matteis, F.; Prosposito, P.; Pizzoferrato, R. *Appl. Phys. Lett.* **1999**, *75*, 2172.
(166) Prosposito, P.; Casalboni, M.; De Matteis, F.; Glasbeek, M.; Quatela, A.; van Veldhoven, E.; Zhang, H. *J. Lumin.* **2001**, *94*−*95*, 623.
(167) Prosposito, P.; Casalboni, M.; De Matteis, F.; Quatela, A.; Glasbeek, M.; van Veldhoven, E.; Zhang, H. *J. Sol-Gel Sci. Technol.* **2003**, *26*, 909.
(168) Reynolds, G. A.; Drexhage, K. H. *Opt. Commun.* **1975**, *13*, 222.
(169) Jones, G., II; Jackson, W. R.; Kanoktanaporn, S.; Halpern, A. M. *Opt. Commun.* **1980**, *33*, 315.
(170) Jones, G., II; Jackson, W. R.; Choi, C.; Bergmark, W. R. *J. Phys. Chem.* **1985**, *89*, 294.
(171) Maroncelli, M.; Kumar, P. V.; Papazyan, A.; Horng, M. L.; Rosenthal, S. J.; Fleming, G. R. Ultrafast Reaction Dynamics and Solvent Effects. *AIP Conf. Proc.* **1994**, *298*, 310.
(172) Kovalenko, S. A.; Ruthman, J.; Ernsting, N. P. *Chem. Phys. Lett.* **1997**, *271*, 40.
(173) McCarthy, P. K.; Blanchard, G. J. *J. Phys. Chem.* **1993**, *97*, 12205.
(174) Jiang, Y.; McCarthy, P. K.; Blanchard, G. J. *Chem. Phys.* **1994**, *183*, 249.
(175) Lewis, J. E.; Maroncelli, M. *Chem. Phys. Lett.* **1998**, *282*, 197.
(176) Gustavsson, T.; Cassara, L.; Gulbinas, V.; Gurzadyan, G.; Mialocq, J.-C.; Pommeret, S.; Sorgius, M.; van der Meulen, P. *J. Phys. Chem. A* **1998**, *102*, 4229.
(177) Shirota, H.; Castner, E. W., Jr. *J. Chem. Phys.* **2000**, *112*, 2367.
(178) Maroncelli, M.; Fleming, G. R. *J. Chem. Phys.* **1988**, *89*, 5044.
(179) Datta, A.; Pal, S. K.; Mandal, D.; Bhattacharyya, K. *J. Phys. Chem. B* **1998**, *102*, 6114.
(180) Sarkar, N.; Das, K.; Datta, A.; Das, S.; Bhattacharyya, K. *J. Phys. Chem.* **1996**, *100*, 15483.
(181) Bart, E.; Meltsin, A.; Huppert, D. *Chem. Phys. Lett.* **1992**, *200*, 592.
(182) Bart, E.; Meltsin, A.; Huppert, D. *J. Phys. Chem.* **1994**, *98*, 3295.
(183) Bart, E.; Meltsin, A.; Huppert, D. *J. Phys. Chem.* **1994**, *98*, 10819.
(184) Chapman, C. F.; Maroncelli, M. *J. Phys. Chem.* **1991**, *95*, 9095.
(185) Karmakar, R.; Samanta, A. *J. Phys. Chem. A* **2002**, *106*, 4447.
(186) Karmakar, R.; Samanta, A. *J. Phys. Chem. A* **2002**, *106*, 6670.
(187) Argaman, R.; Huppert, D. *J. Phys. Chem. A* **1998**, *102*, 6215.
(188) Krolicki, R.; Jarzeba, W.; Mostafavi, M.; Lampre, I. *J. Phys. Chem. A* **2002**, *106*, 1708.
(189) Molotsky, T.; Huppert, D. *J. Phys. Chem. A* **2002**, *106*, 8525.
(190) Levinger, N. E. *Curr. Opin. Colloid Interface Sci.* **2000**, *5*, 118.
(191) Pant, D.; Levinger, N. E. *Langmuir*, **2000**, *16*, 10123.
(192) Willard, D. M.; Levinger, N. E. *J. Phys. Chem. B* **2000**, *104*, 11075.
(193) Riter, R. E.; Wilard, D. M.; Levinger, N. E. *J. Phys. Chem. B* **1998**, *102*, 2705.
(194) Kang, T. J.; Ohta, K.; Tominaga, K.; Yoshihara, K. *Chem. Phys. Lett.* **1998**, *287*, 29.
(195) Tang, C. W.; van Slyke, S. A.; Chen, C. H. *J. Appl. Phys.* **1989**, *65*, 3610.
(196) Kido, J.; Kimura, M.; Nagai, K. *Science* **1995**, *267*, 1332.
(197) Burrows, P. E.; Shen, Z.; Bulovic, V.; McCarty, D. M.; Forrest, S. R.; Cronin, J. A.; Thompson, M. E. *J. Appl. Phys.* **1996**, *79*, 7991.
(198) Sheats, J. R.; Antoniadis, H.; Hueschen, M.; Leonard, W.; Miller, J.; Moon, R.; Roitman, D.; Stocking, A. *Science* **1996**, *273*, 884.
(199) Shaheen, S. E.; Jabbour, G. E.; Kippelen, B.; Peyghambarian, N.; Anderson, J. D.; Marder, S. R.; Armstrong, N. R.; Bellmann, E.; Grubbs, R. H. *J. Appl. Phys.* **1999**, *86*, 2642.
(200) Ballardini, R.; Varani, G.; Indelli, M. T.; Scandola, F. *Inorg. Chem.* **1986**, *25*, 3858.
(201) Walser, A. D.; Sokolik, I.; Priestley, R.; Dorsinville, R. *Synth. Met.* **1997**, *84*, 877.
(202) Sokolik, I.; Walser, A. D.; Priestley, R.; Tang, C. W.; Dorsinville, R. *Synth. Met.* **1997**, *84*, 921.
(203) Lin, L.-J.; Jenekhe, S. A.; Young, R. H.; Borsenberger, P. M. *Appl. Phys. Lett.* **1997**, *70*, 2052.
(204) Stampor, W.; Kalinowski, J.; Marconi, G.; Di Marco, P.; Fattori, V.; Giro, G. *Chem. Phys. Lett.* **1998**, *283*, 373.
(205) Curioni, A.; Boero, M.; Andreoni, W. *Chem. Phys. Lett.* **1998**, *294*, 263.
(206) Ballardini, R.; Varani, G.; Indelli, M. T.; Scandola, F. *Inorg. Chem.* **1986**, *25*, 3858.
(207) Humbs, W.; van Veldhoven, E.; Zhang, H.; Glasbeek, M. *Chem. Phys. Lett.* **1999**, *304*, 10.
(208) Humbs, W.; Zhang, H.; Glasbeek, M. *Chem. Phys.* **2000**, *254*, 319.
(209) van Veldhoven, E.; Zhang, H.; Glasbeek, M. *J. Phys. Chem. A* **2001**, *105*, 1687.
(210) Damrauer, N. H.; Cerullo, G.; Yeh, A.; Boussie, T. R.; Shank, C. V.; McCusker, J. K. *Science* **1997**, *275*, 54.
(211) Sundström, V. *Prog. Quantum Electron.* **2000**, *24*, 187.
(212) Sundström, V.; Gillbro, T. *J. Chem. Phys.* **1984**, *81*, 3463.

(213) Wise, F. W.; Rosker, M. J.; Tang, C. *J. Chem. Phys.* **1987**, *86*, 2827.
(214) Ben-Amotz, D.; Jeanloz, R.; Harris, C. B. *J. Chem. Phys.* **1987**, *86*, 6119.
(215) Martin, M. M.; Plaza, P.; Meyer, Y. H. *J. Phys. Chem.* **1991**, *95*, 9310.
(216) Jurczok, M.; Plaza, P.; Martin, M. M.; Rettig, W. *J. Phys. Chem. A* **1999**, *103*, 3372.
(217) Conrad, R. H.; Heitz, J. R.; Brand, L. *Biochemistry* **1970**, *9*, 1540.
(218) Steiner, R. F.; Albaugh, S.; Nenortas, E.; Norris, L. *Biopolymers* **1992**, *32*, 73.
(219) Oster, G.; Nishijima, Y. *J. Am. Chem. Soc.* **1956**, *78*, 1581.
(220) Changenet, P.; Zhang, H.; van der Meer, M. J.; Glasbeek, M.; Plaza, P.; Martin, M. M. *J. Phys. Chem. A* **1998**, *102*, 6716.
(221) van der Meer, M. J.; Zhang, H.; Glasbeek, M. *J. Chem. Phys.* **2000**, *112*, 2878.
(222) Changenet, P.; Zhang, H.; van der Meer, M. J.; Glasbeek, M.; Plaza, P.; Martin, M. M. *J. Fluoresc.* **2000**, *10*, 155.
(223) Förster, T.; Hoffmann, G. J. *Z. Phys. Chem. (Munich)* **1971**, *75*, 63.
(224) Bagchi, B.; Fleming, G. R.; Oxtoby, D. W. *J. Chem. Phys.* **1983**, *78*, 7375.
(225) Glasbeek, M.; Zhang, H.; Changenet, P.; Plaza, P.; Martin, M. M.; Rettig, W. In *Femtochemistry*; De Schryver, F. C., De Feyter, S., Schweitzer, G., Eds.; Wiley-VCH: Weinheim, Germany, 2001; pp 417−430.
(226) Hirose, Y.; Yui, H.; Fujinami, M.; Sawada, T. *Rev. Sci. Instrum.* **2003**, *74*, 898.
(227) Furui, G.; Ito, K.; Tsuyumoto, I.; Harata, A.; Sawada, T. *J. Phys. Chem. A* **1999**, *103*, 7575.
(228) Van Veldhoven, E.; Zhang, H.; Rettig, W.; Brown, R. G.; Hepworth, J. D.; Glasbeek, M. *Chem. Phys. Lett.* **2002**, *363*, 189.
(229) Van Veldhoven, E.; Zhang, H.; Glasbeek, M. In *Ultrafast Phenomena XIII*; Miller, R. D., Murnane, M. M., Scherer, N. F., Weiner, A. M., Eds.; Springer Series in Chemical Physics, Springer: Berlin (Germany), Vol. 71; 2003; pp 450−452.
(230) Du, M.; Fleming, G. R. *Biophys. Chem.* **1993**, *48*, 101.
(231) Fonseca, T.; Kim, H. J.; Hynes, J. T. *J. Mol. Liq.* **1994**, *60*, 161.
(232) Fonseca, T.; Kim, H. J.; Hynes, J. T. *J. Photochem. Photobiol., A* **1994**, *82*, 67.
(233) Kim, H. J.; Hynes, J. T. *J. Photochem. Photobiol., A* **1997**, *105*, 337.
(234) Nordio, P. L.; Polimeno, A.; Saielli, G. *J. Photochem. Photobiol., A* **1997**, *105*, 269.
(235) Singh, A. K.; Palit, D. K.; Mittal, J. P. *Res. Chem. Intermed.* **2001**, *27*, 125.
(236) Su, S.-G.; Simon, J. D. *J. Phys. Chem.* **1989**, *93*, 753.
(237) Unger, V. M.; Hargrave, P. A.; Baldwin, J. M.; Schertler, G. F. X. *Nature* **1997**, *389*, 203.
(238) Stenkamp, R. E.; Teller, D. C.; Palczewski, K. *ChemBioChem* **2002**, *3*, 963.
(239) Ernst, O. P.; Bartl, F. J. *ChemBioChem* **2002**, *3*, 968.
(240) Haupts, U.; Tittor, J.; Oesterhelt, D. *Annu. Rev. Biophys. Biomol. Struct.* **1999**, *28*, 367.
(241) Quail, P.; Boylan, M. T.; Parks, B. M.; Short, T. W.; Xu, Y.; Wagner, D. *Science* **1995**, *268*, 675.
(242) Andel, F.; Hasson, K. C.; Gai, F.; Anfinrud, P. A.; Mathies, R. A. *Biospectroscopy* **1997**, *3*, 421.
(243) Kochendoerfer, G. G.; Mathies, R. A. *Isr. J. Chem.* **1996**, *35*, 211.
(244) Hellingwerf, K. J.; Hendriks, J.; Gensch, T. *J. Phys. Chem. A* **2003**, *107*, 1082.
(245) Changenet, P.; Zhang, H.; van der Meer, M. J.; Hellingwerf, K. J.; Glasbeek, M. *Chem. Phys. Lett.* **1998**, *282*, 276.
(246) Meyer, T. E. *Biochim. Biophys. Acta* **1985**, *806*, 175.
(247) Hoff, W. D.; Dux, P.; Hard, K.; Devreese, B.; Nugteren-Roodzant, I. M.; Crielaard, W.; Boelen, R.; Kaptein, R.; van Beeumen, J.; Hellingwerf, K. J. *Biochemistry* **1994**, *33*, 13959.
(248) Baca, M.; Borgstahl, G. E. O.; Boissinot, M.; Burke, P. M.; Williams, D. R.; Slater, K. A.; Getzoff, E. D. *Biochemistry* **1994**, *33*, 14369.
(249) Hoff, W. D.; Devreese, B.; Fokkens, R.; Nugteren-Roodzant, I. M.; van Beeumen, J.; Nibbering, N. M. M.; Hellingwerf, K. J. *Biochemistry* **1996**, *35*, 1274.
(250) Kim, M.; Mathies, R. A.; Hoff, W. D.; Hellingwerf, K. J. *Biochemistry* **1995**, *34*, 12669.
(251) Meyer, T. E.; Tollin, G.; Causgrove, T. P.; Cheng, P.; Blankenship, R. E. *Biophys. J.* **1991**, *59*, 988.
(252) Chosrowjan, H.; Mataga, N.; Nakashima, N.; Imamoto, Y.; Tokunaga, F. *Chem. Phys. Lett.* **1997**, *270*, 267.
(253) Haran, G.; Wynne, K.; Xie, A.; He, Q.; Chance, M.; Hochstrasser, R. M. *Chem. Phys. Lett.* **1996**, *261*, 389.
(254) Hasson, K. C.; Gai, F.; Anfinrud, P. A. *Proc. Natl. Acad. Sci. U.S.A.* **1996**, *93*, 15124.
(255) Van der Meer, M. J.; Zhang, H.; Hellingwerf, K. J.; Glasbeek, M. Unpublished results.
(256) Xie, A.; Hoff, W. D.; Kroon, A. R.; Hellingwerf, K. J. *Biochemistry* **1996**, *35*, 14671.
(257) Imamoto, Y.; Mihara, K.; Hisatomi, O.; Katoaka, M.; Tokunaga, F.; Bojkova, N.; Yoshihara, K. *J. Biol. Chem.* **1997**, *272*, 12905.
(258) Genick, U. K.; Soltis, S. M.; Kuhn, P.; Canestrelli, I. L.; Getzoff, E. D. *Nature* **1998**, *392*, 206.
(259) Chosrowjan, H.; Mataga, N.; Shibata, Y.; Imamoto, Y.; Tokunaga, F. *J. Phys. Chem. B* **1998**, *102*, 7695.
(260) Mataga, N.; Chosrowjan, H.; Shibata, Y.; Imamoto, Y.; Tokunaga, F. *J. Phys. Chem. B* **2000**, *104*, 5191.
(261) Mataga, N.; Chosrowjan, H.; Shibata, Y.; Imamoto, Y.; Kataoka, M.; Tokunaga, F. *Chem. Phys. Lett.* **2002**, *352*, 220.
(262) Changenet-Barret, P.; Plaza, P.; Martin, M. M. *Chem. Phys. Lett.* **2001**, *336*, 439.
(263) Changenet-Barret, P.; Espagne, A.; Katsonis, N.; Charier, S.; Baudin, J.-B.; Jullien, L.; Plaza, P.; Martin, M. M. *Chem. Phys. Lett.* **2002**, *365*, 285.
(264) Kandori, H.; Furutani, Y.; Nishimura, S.; Shichida, Y.; Chosrowjan, H.; Shibata, Y.; Mataga, N. *Chem. Phys. Lett.* **2001**, *334*, 271.
(265) Weidlich, O.; Ujj, L.; Jäger, F.; Atkinson, G. H. *Biophys. J.* **1997**, *72*, 2329.
(266) Atkinson, G. H.; Zhou, Y.; Ujj, L.; Aharoni, A.; Sheves, M.; Ottolenghi, M. *J. Phys. Chem. A* **2002**, *106*, 3325.
(267) Mandal, D.; Tahara, T.; Webber, N. M.; Meech, S. R. *Chem. Phys. Lett.* **2002**, *358*, 495.
(268) Rüdiger, W.; Thümmler, F. *Angew. Chem., Int. Ed. Engl.* **1991**, *30*, 1216.
(269) Teuchner, K.; Schulz-Evers, M.; Stiel, H.; Strehlow, D.; Rüdiger, W. *J. Photochem. Photobiol., B* **1999**, *53*, 115.
(270) Bischoff, M.; Hermann, G.; Rentsch, S.; Strehlow, D. *Biochemistry* **2001**, *40*, 181.
(271) Bischoff, M.; Hermann, G.; Rentsch, S.; Strehlow, D. *J. Phys. Chem. A* **1998**, *102*, 4399.
(272) Zhong, Q.; Ruhman, S.; Ottolenghi, M.; Sheves, M.; Friedman, N.; Atkinson, G. H.; Delaney, J. K. *J. Am. Chem. Soc.* **1996**, *118*, 12828.
(273) Ye, T.; Gershgoren, E.; Friedman, N.; Ottolenghi, M.; Sheves, M.; Ruhman, S. *Chem. Phys. Lett.* **1999**, *314*, 429.
(274) Hou, B.; Friedman, N.; Ruhman, S.; Sheves, M.; Ottolenghi, M. *J. Phys. Chem. B* **2001**, *105*, 7042.
(275) Haran, G.; Morlino, E. A.; Matthes, J.; Callender, R. H.; Hochstrasser, R. M. *J. Phys. Chem. A* **1999**, *103*, 2202.
(276) Huang, Y.; Cheng, T.; Li, F.; Huang, C.-H.; Wang, S.; Huang, W.; Gong, Q. *J. Phys. Chem. B* **2002**, *106*, 10041.
(277) De Belder, G.; Schweitzer, G.; Jordens, S.; Lor, M.; Mitra, S.; Hofkens, J.; De Feyter, S.; Van der Auweraer, M.; Herrmann, A.; Weil, T.; Mullen, K.; De Schryver, F. C. *ChemPhysChem* **2001**, *2*, 49.
(278) Cho, H. S.; Song, N. W.; Kim, Y. H.; Jeoung, S. C.; Hahn, S.; Kim, D.; Kim, S. K.; Yoshida, N.; Osuka, A. *J. Phys. Chem. A* **2000**, 104, 3287.
(279) Mataga, N.; Shibata, Y.; Chosrowjan, H.; Yoshida, N.; Osuka, A. *J. Phys. Chem. B* **2000**, *104*, 4001.
(280) Kim, Y. H.; Jeong, D. H.; Kim, D.; Jeoung, S. C.; Cho, H. S.; Kim, S. K.; Aratani, N.; Osuka, A. *J. Am. Chem. Soc.* **2001**, *123*, 76.
(281) Mataga, N.; Chosrowjan, H.; Shibata, Y.; Tanaka, F.; Nishina, Y.; Shiga, K. *J. Phys. Chem. B* **2000**, *104*, 10667.
(282) Zimmer, M. *Chem. Rev.* **2002**, *102*, 759.
(283) Stubner, M.; Schellenberg, P. *J. Phys. Chem. A* **2003**, *107*, 1246.
(284) Litvinenko, K. L.; Webber, N. M.; Meech, S. R. *Bull. Chem. Soc. Jpn.* **2002**, *75*, 1065.
(285) McAnaney, T. B.; Park, E. S.; Hanson, G. T.; Remington, S. J.; Boxer, S. G. *Biochemistry* **2002**, *41*, 15489.
(286) Pal, H.; Shirota, H.; Tominaga, K.; Yoshihara, K. *J. Chem. Phys.* **1999**, *110*, 11454.
(287) Rubtsov, I. V.; Shirota, H.; Yoshihara, K. *J. Phys. Chem. A* **1999**, *103*, 1801.
(288) Rubtsov, I. V.; Yoshihara, K. *J. Phys. Chem. A* **1999**, *103*, 10202.
(289) Castner, E. W., Jr.; Kennedy, D.; Cave, R. J. *J. Phys. Chem. A* **2000**, *104*, 2869.
(290) Iwai, S.; Murata, S.; Katoh, R.; Tachiya, M.; Kikuchi, K.; Takahashi, Y. *J. Chem. Phys.* **2000**, *112*, 7111.
(291) Kononov, A. I.; Moroshkina, E. B.; Tkachenko, N. V.; Lemmetyinen, H. *J. Phys. Chem. B* **2001**, *105*, 535.
(292) Tachibana, Y.; Rubtsov, I. V.; Montanari, I.; Yoshihara, K.; Klug, D. R.; Durrant, J. R. *J. Photochem. Photobiol., A* **2001**, *142*, 215.
(293) Underwood, D. F.; Kippeny, T.; Rosenthal, S. J. *J. Photochem. Photobiol., B* **2001**, *105*, 436.
(294) Link, S.; El-Sayed, M. A.; Schaaff, T. G.; Whetten, R. L. *Chem. Phys. Lett.* **2002**, *356*, 240.
(295) Brunsveld, L.; Zhang, H.; Glasbeek, M.; Vekemans, J. A. J. M.; Meijer, E. W. *J. Am. Chem. Soc.* **2000**, *122*, 6175.
(296) Toele, P.; Zhang, H.; Trieflinger, C.; Daub, J.; Glasbeek, M. *Chem. Phys. Lett.* **2003**, *368*, 66.

CR0206723